ABSTRACT

CHEN, YU. Development of Single-Walled Carbon Nanotube-Based Optical Sensors (Under the direction of Dr. Januka Budhathoki-Uprety).

Sensor materials that facilitate sensitive and specific measurements with high accuracy and convenience of detection are in high demand for disease detection, diagnosis and improve clinical outcome. Single-walled carbon nanotube (SWCNT), which is a one cylinder of graphene sheet, has potential for biosensor development due to its extraordinary optical and electronic properties. In this research, we measured the photoluminescence of SWCNTs dispersed with different surfactants and their optical response to different polymers including biologically relevant molecules. We found that SWCNT dispersed with molecules containing sulfonate/sulfonic acid groups exhibited a fluorescence enhancement upon addition of cationic polymers. Based on this observation, we designed an optical sensor for protamine which is a biomarker in many biological processes, using poly(sodium 4-styrenesulfonate) (PSS)- wrapped (6,5) SWCNT. This polymer-SWCNT complex produced a strong fluorescence enhancement upon binding with protamine. The electrostatic interaction between the positively charged polymer and negatively charged dispersant molecules most likely causes displacement of water molecules from carbon nanotube surface resulting in fluorescence enhancement.

Development of Single-Walled Carbon Nanotube-Based Optical Sensors

by
Yu Chen

A thesis submitted to the Graduate Faculty of
North Carolina State University
in partial fulfillment of the
requirements for the degree of
Master of Science

Textile Chemistry

Raleigh, North Carolina
2020

APPROVED BY:

Dr. Januka Budhathoki-Uprety Committee Chair	Dr. Peter Hauser
Dr. Yingjiao Xu	

DEDICATION

This study is wholeheartedly dedicated to my family, who encourage me, accompany me, and support me throughout my whole life. I would not be here without you all.

To my dear advisor Dr. Januka Budhathoki-Uprety, you showed me how great a professor could be, and you gave me the motivation to continue my PhD study.

BIOGRAPHY

Yu Chen was born and raised in Hui Zhou, Guangdong province China. He got his Bachelor of Science in Dyeing & Finishing Engineering at Jangnan University in Wuxi, Jiangsu province. After that he joined North Carolina State University in 3+X program at Wilson College of Textiles. In 2019 he was accepted to the Master of Science in Textile Chemistry Program in Wilson college of Textiles. He worked under the supervision of Dr. Januka Budhathoki-Uprety and concentrated on the study of single-walled carbon nanotubes as optical sensor development.

ACKNOWLEDGMENTS

I want to sincerely thank my committee chair, Dr. Januka Budhathoki-Uprety for guiding me my first research project in the United States. Your support and guidance throughout the research and writing process has been invaluable. You made me feel the charm of scientific research and inspired me to go further on this path.

Thank you to all my committee members for your valuable advice and support.

Thank you to Nigar Sultana, Nidhi Godthi, Hannah Dewey and all lab members for your assistance and time supporting the development of this research.

Thank you to Birgit Andersen for your technical assistance in the Analytical Lab. Thank you Dr. Gluck for giving me a lot information about biomarkers.

I want to thank all the friends and people who support and help me during my studying and living in the United States.

TABLE OF CONTENTS

LIST OF FIGURES. viii

Chapter 1: INTRODUCTION 1

Chapter 2: LITERATURE REVIEW 3

2.1. Structure of SWCNT 3

2.2. SWCNT Fluorescence 4

2.3. Synthesis of SWCNT 6

2.4. Purification of SWCNT 7

2.5. Dispersion of SWCNT 8

2.5.1. Covalent Functionalization 9

2.5.2. Non-covalent Functionalization 11

2.6. SWCNT as Optical Sensor 16

2.7. Protamine and Its Detection 22

Chapter 3: EXPERIMENTAL METHOD AND MATERIAL 26

3.1. Material and General Method 26

3.2. Fluorescence measurement of surfactant-SWCNT systems 27

3.2.1. Preparation of sodium cholate (SC)-(7,6) SWCNT and fluorescence measurement 27

3.2.2. Preparation of sodium cholate (SC)-(6,5) SWCNT and fluorescence measurement 27

3.2.3. Preparation of sodium dodecyl sulfate (SDS)-(7,6) SWCNT and fluorescence measurement 28

3.2.4. Preparation of sodium dodecyl sulfate (SDS)-(6,5) SWCNT and fluorescence measurement 28

3.2.5. Preparation of sodium dodecylbenzenesulfonate (SDBS)-(7,6) SWCNT and fluorescence measurement 29

3.2.6. Preparation of sodium laurate- (7,6) SWCNT and fluorescence measurement 29

3.3. Effect of poly(diallyldimethylammonium chloride) (PDADMAC) on surfactant-SWCNT systems 30

3.3.1. Effect of PDADMAC on SC- (7,6) SWCNT 30

3.3.2. Effect of PDADMAC on SC- (6,5) SWCNT 30

3.3.3. Effect of PDADMAC on SDS- (7,6) SWCNT 30

3.3.4. Effect of PDADMAC on SDS- (6,5) SWCNT 30

3.3.5. Effect of PDADMAC on SDBS- (7,6) SWCNT 31

3.3.6. Effect of PDADMAC on Sodium laurate- (7,6) SWCNT 31

3.4. Effect of poly(allylamine hydrochloride) (PAH) on surfactant-SWCNT systems 31
3.4.1. Effect of PAH on SC- (7,6) SWCNT 31
3.4.2. Effect of PAH on SC- (6,5) SWCNT 31
3.4.3. Effect of PAH on SDS- (7,6) SWCNT 32
3.4.4. Effect of PAH on SDS- (6,5) SWCNT 32
3.4.5. Effect of PAH on SDBS- (7,6) SWCNT 32
3.4.6. Effect of PAH on Sodium laurate- (7,6) SWCNT 32
3.5. Effect of poly acrylic acid(PAA) on surfactant- SWCNT systems 33
3.5.1. Effect of PAA on SDBS- (7,6) SWCNT 33
3.5.2. Effect of PAA on Sodium laurate- (7,6) SWCNT 33
3.6. Preparation of PSS- SWCNT 33
3.6.1. Effect of PDADMAC on PSS- (6,5) SWCNT 34
3.6.2. Effect of PAH on PSS- (6,5) SWCNT 34
3.6.3. Effect of protamine on PSS- (6,5) SWCNT 34
3.6.3.1. Protamine concentration (0-2500mg/L) 34
3.6.3.2. Protamine concentration (0-1000mg/L) 35
3.6.3.3. Protamine concentration (1000mg/L) 35
3.6.3.4. Protamine concentration (0-30mg/L) 35
3.6.4. Kinetics experiment of protamine addition to PSS- (6,5) SWCNT 35
3.6.5. PSS- (6,5) SWCNT with 0.02% PDADMAC, PAH and protamine solution 35
3.6.6. PAA- (6,5) SWCNT with 0.02% PDADMAC, PAH and protamine solution 36
Chapter 4: RESULTS AND DISCUSSION 37
4.1. Fluorescence of surfactant-SWCNT system 37
4.2. Effect of poly(diallyldimethylammonium chloride) (PDADMAC) on surfactant-SWCNT systems 40
4.2.1. Effect of PDADMAC on SC- (7,6) SWCNT and SC-(6,5) SWCNT 40
4.2.2. Effect of PDADMAC on SDS- (7,6) SWCNT and SDS-(6,5) SWCNT 41
4.2.3. Effect of PDADMAC on SDBS- (7,6) SWCNT and sodium laurate-(7,6) SWCNT 43
4.3. Effect of poly(allylamine hydrochloride) (PAH) on surfactant-SWCNT systems 44
4.3.1. Effect of PAH on SC- (7,6) SWCNT and SC- (6,5) SWCNT 45
4.3.2. Effect of PAH on SDS- (7,6) SWCNT and SDS- (6,5) SWCNT 46
4.3.3. Effect of PAH on SDBS- (7,6) SWCNT and sodium laurate- (7,6) SWCNT 47
4.4. Effect of poly acrylic acid (PAA) on surfactant-SWCNT systems 49

4.4.1. Effect of PAA on SDBS- (7,6) SWCNT and sodium laurate- (7,6) SWCNT 50
4.5. Discussion and Conclusion 51
4.6. PSS- (6,5) SWCNT as an optical sensor 52
4.6.1. Effects of PDADMAC and PAH on PSS- (6,5) SWCNT 54
4.6.2. Effect of protamine on PSS- (6,5) SWCNT 55
4.6.2.1. Protamine concentration (0-2500mg/L) 56
4.6.2.2. Effect of protamine on PSS- (6,5) SWCNT (0-1000mg/L) 57
4.6.2.3. Effect of protamine on PSS- (6,5) SWCNT (1000mg/L) 57
4.6.2.4. Effect of protamine on PSS- (6,5) SWCNT (0-30mg/L) 58
4.6.3. Kinetics experiment of PSS- (6,5) SWCNT with 50mg/L protamine 59
4.6.4. PSS- (6,5) SWCNT with 0.02% PDADMAC, PAH and protamine 60
4.6.5. PAA- (6,5) SWCNT with 0.02% PDADMAC, PAH and protamine 61
4.6.6. Discussion and Conclusion 62
Chapter 5: CONCLUSION AND OUTLOOK 64
REFERENCES 66
Appendices 71
Appendix A 72
Appendix B 73

LIST OF FIGURES

Figure 2.1 Construction of SWCNT structure. 4

Figure 2.2 Electronic structure and fluorescence spectra of semiconducting SWCNTs 5

Figure 2.3 Scheme to produce carbon nanotubes using catalytic chemical vapor deposition 7

Figure 2.4 Purification methods for carbon nanotubes 8

Figure 2.5 Oxidized carbon nanotubes 10

Figure 2.6 Preparation of amino-functionalized SWCNTs 10

Figure 2.7 Modification of SWCNTs via dimethyl acetylenedicarboxylate-4-dimethylaminopyridine zwitterion method 11

Figure 2.8 Cross-section model of SDS suspended SWCNT 12

Figure 2.9 Schematic representation of *N*-succinimidyl-1- pyrenebutanoate-SWCNT 14

Figure 2.10 Possible wrapping construction of PVP on an (8,8) SWCNT 14

Figure 2.11 SWCNT is functionalized with poly(ethylene glycol) (PL-PEG). 15

Figure 2.12 Preparation of DNA-SWCNT 17

Figure 2.13 (6,5) SWCNT fluorescence change after addition of cDNA 17

Figure 2.14 Mechanism of SWCNT sensor for miRNA 18

Figure 2.15 SWCNT sensor for albumin detection 19

Figure 2.16 Interaction of Serotonin (5HT) with serotonin nano-sensor NIRSer 20

Figure 2.17 Construction and mechanism of SWCNT/protein microarray 20

Figure 2.18 Photoluminescence spectra of DNA-SWCNT nanosensors upon addition of DNA-intercalating agents 21

Figure 2.19 Detection of protamine and trypsin by MPA-AgInZnS quantum 25

Figure 2.20 Photoluminescence spectra of AIZS QDs, AIZS QDs/protamine 25

Figure 4.1 Structure of surfactants 38

Figure 4.2 Fluorescence of (a) SC-(7,6) SWCNT, (b) SC-(6,5) SWCNT, (c) SDS-(7,6) SWCNT, (d) SDS-(6,5) SWCNT, (e)SDBS-(7,6) SWCNT and (f) Sodium laurate-(7,6) SWCNT 39

Figure 4.3 Structure of PDADMAC 40

Figure 4.4 Effect of PDADMAC addition on SC-(7,6) SWCNT fluorescence 41

Figure 4.5 Effect of PDADMAC addition on SC-(6,5) SWCNT fluorescence 41

Figure 4.6 Effect of PDADMAC addition on SDS-(7,6) SWCNT fluorescence 42

Figure 4.7 Effect of PDADMAC addition on SDS-(6,5) SWCNT fluorescence 43

Figure 4.8 Effect of PDADMAC addition on Sodium laurate-(7,6) SWCNT fluorescence 44

Figure 4.9 Effect of PDADMAC addition on SDBS-(7,6) SWCNT fluorescence 44

Figure 4.10 Structure of PAH 45

Figure 4.11 Effect of PAH addition on SC-(7,6) SWCNT fluorescence 46

Figure 4.12 Effect of PAH addition on SC-(6,5) SWCNT fluorescence 46

Figure 4.13 Effect of PAH addition on SDS-(7,6) SWCNT fluorescence 47

Figure 4.14 Effect of PAH addition on SDS-(6,5) SWCNT fluorescence 47

Figure 4.15 Effect of PAH addition on SDBS-(7,6) SWCNT fluorescence 48

Figure 4.16 Effect of PAH addition on Sodium laurate-(7,6) SWCNT fluorescence 49

Figure 4.17 Structure of Poly(acrylic acid sodium salt). 50

Figure 4.18 Effect of PAA addition on SDBS-(7,6) SWCNT fluorescence 50

Figure 4.19 Effect of PAA addition on Sodium laurate-(7,6) SWCNT fluorescence 51

Figure 4.20 Scheme for the mechanism of the fluorescence enhancement and quenching of surfactant- SWCNT upon the addition of cationic polymers. 53

Figure 4.21 Structure of Poly(sodium 4-styrenesulfonate). 54

Figure 4.22 Effect of PDADAC on PSS-(6,5) SWCNT fluorescence. 55

Figure 4.23 Effect of PAH on PSS-(6,5) SWCNT fluorescence. 55

Figure 4.24 Effect of protamine (0-2500mg/L) on PSS-(6,5) SWCNT fluorescence. 56

Figure 4.25 Effect of protamine (0-1000mg/L) on PSS-(6,5) SWCNT fluorescence. 57

Figure 4.26 Representative spectra of PSS-(6,5) SWCNT with 1000mg/L protamine. 58

Figure 4.27 Kinetics experiment of PSS-(6,5) SWCNT with 50mg/L protamine 59

Figure 4.28 Effect of protamine (0-30mg/L) on PSS-(6,5) SWCNT fluorescence. 60

Figure 4.29 Representative spectra of PSS-(6,5) SWCNT after addition of 100μL 0.02% PDADMAC, 0.02% PAH and 0.02% protamine solution 61

Figure 4.30 Representative spectra of PAA-(6,5) SWCNT after addition of 100μL 0.02% PDADMAC, 0.02% PAH and 0.02% protamine solution. 62

Figure 4.31 Scheme for the mechanism of fluorescence enhancement of PSS- SWCNT upon the addition of a cationic polymer..... 63

CHAPTER 1

INTRODUCTION

Biosensor is a sensor that can quantitatively analyze the target in the biological environment, and it has very important scientific significance in the biological and medical fields[1]. A biosensor, generally consists of at least two parts, one is a unit that can identify the target, and the other is a unit that can convert the recognition into an observable signal[2]. In order to improve the accuracy and convenience of detection and improve clinical treatment, new sensor technologies such as point-of-care devices have gained much attention[3 4]. Nanomaterials such as nanoparticles, graphene and carbon nanotubes are widely studied due to their unique physical and chemical properties[3]. As a low-dimensional material compared with three-dimensional materials, these nanomaterials have strong selectivity and sensitivity and can minimize the impact on the biological environment, which makes them a good platform for biosensors[5]. Currently, there is a lot of research being conducted on nanomaterial-based biosensors.

Carbon nanotube was first reported by Sumio Iijima in 1991[6]. Two years later, buckytubes (single-walled carbon nanotubes) were observed[7]. Single wall carbon nanotubes (SWCNTs) can be considered as one cylinder of graphene sheet, which are fully composed of sp^2 hybridized carbon[8]. It is a one-dimensional nanomaterial with a diameter range from 0.8 and 1.2 nm. Although it consists entirely of carbon atoms, SWCNTs have different structures and diameter. People commonly used (*n*,*m*), as their chirality, to distinguish these structures[9]. According to their chirality and dimension, SWCNTs exhibit exceptional optical and electrical properties that differ in function[10]. Thus, SWCNT can be designed as electrochemical sensors, mechanical sensors and optical sensors.

SWCNTs have photoluminescence (PL) in near-infrared (NIR) range, which is tunable, stable, penetrable and detectable, particularly for *in vivo* applications[10]. The emission from SWCNTs is so sensitive that it can be used to detect analytes such as protein, peptides, and small ions that are inside body[11]. At the same time, its huge surface area ratio makes it possible to functionalize on its surface which allow applications such as subcellular targeting, drug delivery and sensor[12]. Because of their unique properties, it attracts many attentions in different fields, especially in biomedicine.

Here we will mainly focus on SWCNTs as optical biosensors due to their excellent biocompatibility and photosensitivity. In this chapter, a brief introduction to SWCNTs and its properties, and methods of carbon nanotube suspension preparation are discussed. Then, some examples of SWCNTs as optical sensors and the application prospects of carbon nanotubes are presented.

CHAPTER 2

LITERATURE REVIEW

2.1. Structure of SWCNT

Carbon nanotubes can be thought of as rolled up graphene sheets with high aspect ratio, which consists of sp2-hybridized carbon atoms that have σ-bonds to three nearest neighbors. In each end of the nanotube there is a hemi-fullerene cap. Due to the high aspect ratio, these "caps" only have an insignificant effect on nanotubes property[10]. Although all nanotubes are composed of carbon atoms, their physical and chemical properties are different because of their structure. As mentioned above, nanotubes are rolled-up graphene. Thus, each nanotube has a special diameter and rolled-up angle. Commonly, chiral index (*n,m*) was given to represent the structure. Figure 2.1 explained what a chiral index is. Basically, the rolled-up vector, C_h, is the circumference of nanotube and $C_h = na_1+ma_2 = (n,m)$, a_1 and a_2 is the initial lattice vector. The range of chiral indexes is from (n,0) to (n,n). (n,0) means the roll-up angle is 0° which is also called "zigzag". (n,n) is when the roll-up angle is 30° and is named "armchiral". As $C_h = na_1+ma_2 = (n,m)$, where $a \equiv |a_1| = |a_2| = \sqrt{3}\, a_{C-C}$, therefore the diameter for a given (n,m) will be

$d= |C_h|/\pi = (a\sqrt{n2 + nm + m2})/\pi$[13]

The roll-up or chiral angle is given by

$a= \tan^{-1}(\sqrt{3}*m/(2n=m)$[13]

a is the graphene lattice constant which is 0.0246nm. The SWCNTs will be metallic if n-m=0, or be semi-metallic if (n-m)/3 is an integer, and other chirality will be the semiconducting[14].

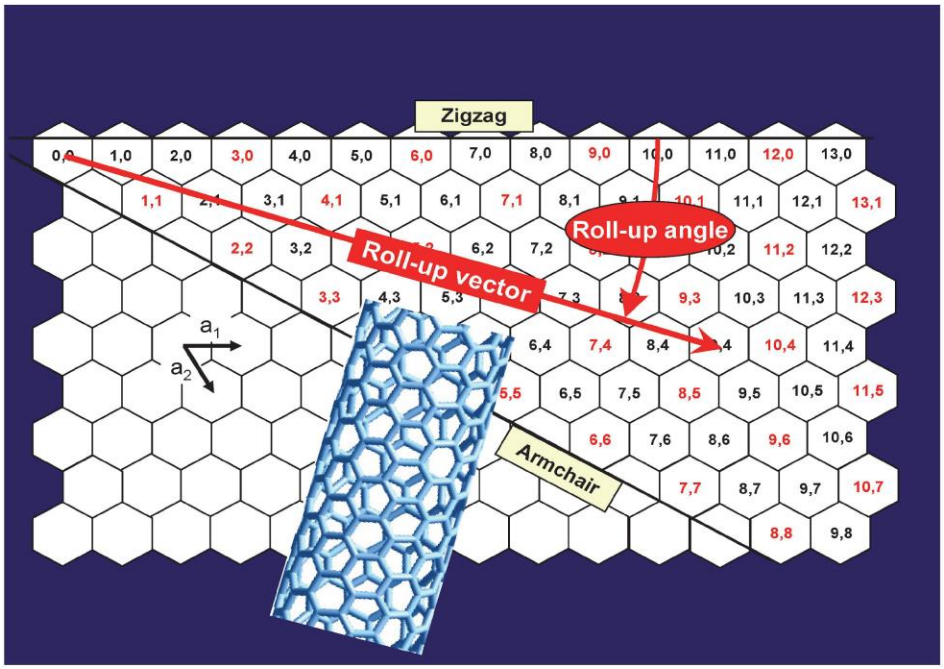

Figure 2.1 Construction of SWCNT structure. a_1 and a_2 are primitive lattice vectors. When the graphene sheet roll-up from (0,0) to a cell (*n*,*m*) and becomes nanotubes, the roll-up vector is the circumference[13].

2.2. SWCNT Fluorescence

Before the introduction of single-walled carbon nanotube based optical sensor, it is necessary to understand the mechanism of nanotubes fluorescence, which is related to their electrical property and photophysical behavior. As mentioned above, SWCNT can mainly be divided into two characteristics: metallic SWCNT and semiconducting SWCNT[13]. Metallic SWCNT has similar properties to metals. There is no energy gap between valence and conduction band. For semiconducting SWCNTs, there are electronic states between valence and conduction bands (Figure 2.2). When a laser or other source of light with matched wavelength is absorbed by semiconducting SWCNTs, there will be an E_{22} transition then followed by E_{11} emission. For most semiconducting SWCNTs, their emission is in the near-infrared spectrum (900-1600nm)[14].

Figure 2.2a illustrates the transition of electrons. For carbon nanotubes, it is the excitons that absorb energy into the excited state. An exciton is an electron/hole pair with a certain Coulombic interaction[10]. The excitons will move through the conjugate system on the surface of SWCNT during photoluminescence/fluorescence[13]. This makes them very sensitive to the electron distribution on the surface of carbon nanotubes. As the surface chemical environment changes, the excitons' movements are also affected, resulting in a change in fluorescence (Figure 2.2c)[13].

SWCNTs have many chiralities. It not only gives different physical structures, but also gives them different band gaps. As shown in figure 2.2b, because of the different absorption wavelengths, SWCNTs have different colors[10]. Various band gaps give SWCNTs different fluorescence peaks in NIR spectrum and thus significant advantage as a biosensor: multiplexing capability, which means it can be used to detect several targets at same time. For example, Jackson D. Harvey et al. used (8,6) and (6,5) SWCNTs, simultaneously and separately, to successfully detect miR-19 RNA and miR-509 RNA[15].

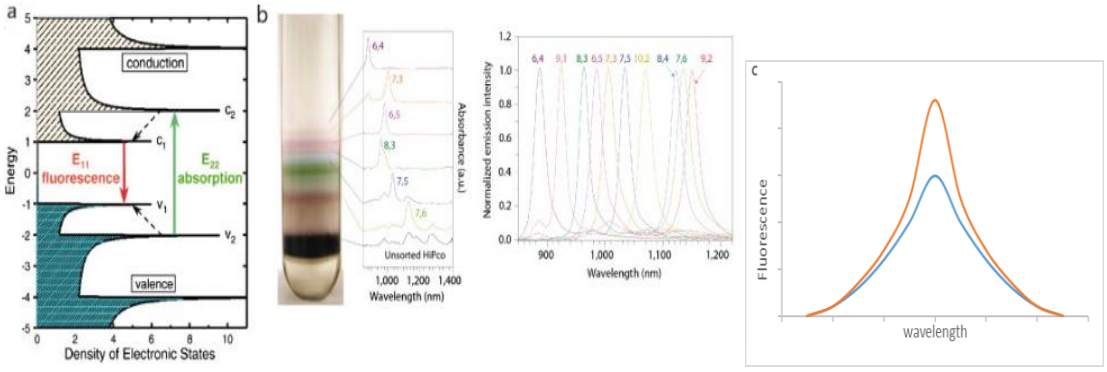

Figure 2.2 Electronic structure and fluorescence spectra of semiconducting single-walled carbon nanotubes: a) Density of electronic states of a semiconducting SWCNT. The van-Hove-singularities arise due to quantum confinement. The most important transitions that are the reason for near-infrared fluorescence are depicted in red (E_{11}) and green (E_{22}). b) Sample with separated SWCNT of different chiralities and corresponding absorption and fluorescence spectra[10]. c) Fluorescence changes with the change of chemical environment.

2.3. Synthesis of SWCNT

Mainly, there are three methods to synthesize carbon nanotubes: (1) the chemical vapor deposition (CVD) technique, (2) the laser-ablation technique, and (3) the carbon arc-discharge technique[16].

Electric arc discharge is the first method used for the synthesis of carbon nanotubes. This method involves two different electrodes, one is high-purity graphite and another one is either graphite or metals[16]. By using direct current to pass through two electrodes, the nanotubes were generated in a gaseous atmosphere[17]. Different metal catalysts were applied to obtain single-walled carbon nanotubes in the chamber soot[18].

The laser vaporization approach was first used by Dr Richard E. Smalley of Rice University to produce multi-walled carbon nanotubes and was successful in producing single-walled nanotubes as well[16]. This method using a laser beam to vaporize the graphite-transition metal composite rod. The reaction was carried out in the presence of inert gas. The diameter of nanotubes can be controlled by changing the reaction temperature.

Chemical vapor deposition (CVD), which is a commonly used method for carbon nanotube synthesis, includes various different approaches such as catalytic chemical vapor deposition (CCVD), water assisted CVD, microwave plasma (MPECVD), radiofrequency CVD (RF-CVD), or hot-filament (HFCVD). Catalytic chemical vapor deposition (CCVD) is the most common method for the production of single-walled carbon nanotubes[19]. Figure 2.3 shows the process to produce carbon nanotubes using catalytic chemical vapor deposition (CCVD). Basically, a hydrocarbon such as acetylene was passed through a silicon tube which has metal catalysis in the holes. The nanotubes were produced upon the contact of carbon and metal particles. Tubes are drilled into silicon and implanted with iron nanoparticles at the bottom. After

that, a hydrocarbon such as acetylene is heated and decomposed onto the substrate. This method usually uses transition metals nickel, copper, or iron as metal nanoparticles, and mixed with catalyst support such as MgO or Al_2O_3 to improve the yield[20].

Currently, low temperature chemical vapor deposition (CVD) technique (less than 800℃) has been used as a dominant method to synthesize SWCNTs because this method can better control the size, diameter and architecture of carbon nanotubes[16].

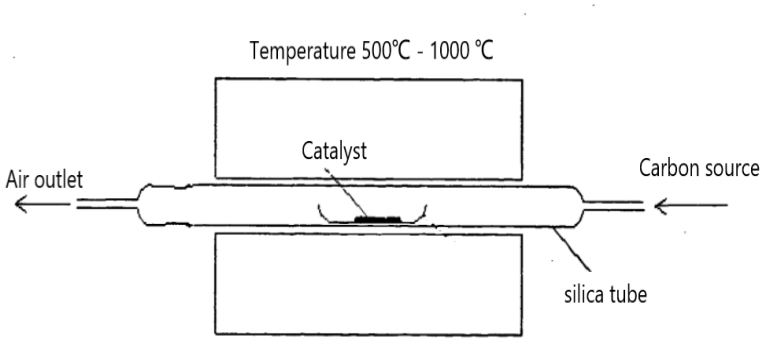

Figure 2.3 Scheme to produce carbon nanotubes using catalytic chemical vapor deposition.

Based on CVD, Dr Richard Smalley's group at Rice University also developed a high pressure carbon monoxide disproportionation (HiPco) method[21]. By adding carbon monoxide (CO) with iron pentacarbonyl ($Fe(CO)_5$) to the reactor and producing iron clusters, carbon nanotubes can generate along the iron clusters.

2.4. Purification of SWCNTs

Impurities of as-synthesized SWCNTs include carbonaceous contaminants and metal catalysts. For carbon nanotubes with purity requirements, the metallic SWCNTs are considered as Impurity as well[19]. Purification has the following main purposes: eliminate polyhedral carbons and graphitic particles, deletion of carbonaceous and metal impurities, and remove remnant catalyst particles and fullerene[19]. For SWCNTs, it may need to remove the residual MWCNTs.

However, according to the different production methods and steps in SWCNTs synthesis, the impurities contained in the produced carbon nanotubes are also different, which makes the purification method various. Compared to the advanced production methods of SWCNTs, there is no general method for carbon nanotube purification. Figure 2.4 shows some common methods for SWCNTs purification[22]. Currently, the available commercial product of SWCNTs can reach more than 90% purity[19].

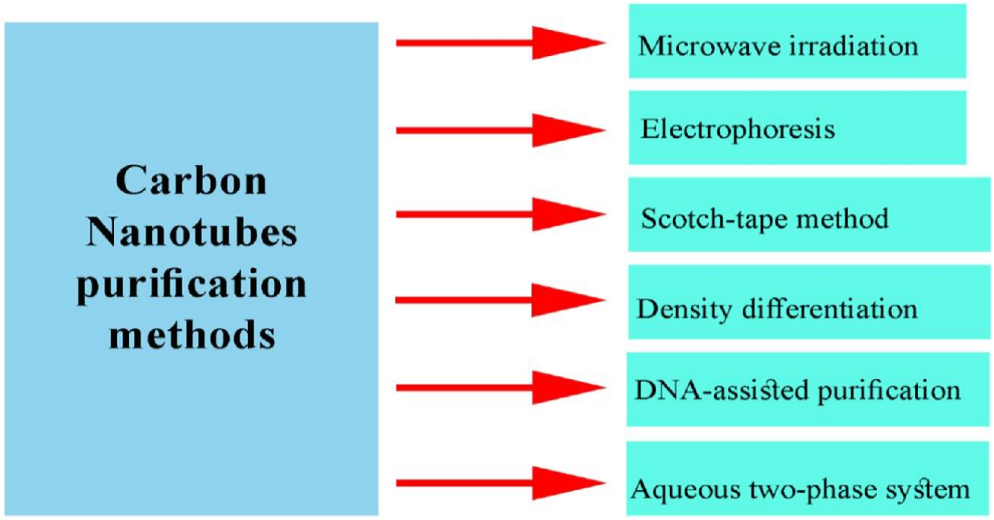

Figure 2.4 Different purification methods of carbon nanotubes[23].

2.5. Dispersion of SWCNT

SWCNTs are insoluble in common solvents and normally exist as bundles or ropes[24] due to strong van der Waals interaction. To apply SWCNTs as optical sensors, nanotubes need to be singly dispersed into suspension. When metallic SWCNTs bundle with semiconducting SWCNTs, it causes fluorescence quench, and weakens optical response[25]. That is because the energy will transfer from semiconducting SWCNTs to metallic SWCNTs, and there is no energy gap between electronic valence bands in metallic SWCNTs[13].

Generally, there are two methods to disperse SWCNT in solution, either by covalent functionalization or noncovalent functionalization[26].

2.5.1. Covalent Functionalization

Generally, covalent functionalization of SWCNTs can be either on the ends or on the sidewalls of the tube[27]. The ends of the tube are semi fullerene-like structures, which have better chemical reactivity compared to the sidewalls. There are many different methods for chemical functionalization of SWCNTs, one of the most common methods is oxidation reaction[28]. SWCNT oxidation can be done on both the sidewalls and the ends of the tube, and the carboxyl group normally generated after reaction[27]. The functional group generated by SWCNT oxidation can be further functionalized. The oxidation of carbon nanotubes usually has the following steps. First is the oxidation on the reactive site such as the defects on the sidewalls. After it, more active sites will be generated after sidewall damage. Then the vacancy will be generated in the graphene layer. This reaction will continue to react on the sidewalls or the ends of the tube, consuming the graphene sidewall around the vacancy and releasing shorter, cut SWCNTs[27].

The oxidation reaction of piranha (H_2SO_4/H_2O_2) solutions onto SWCNTs was reported by Ziegler et al[29]. This treatment generates cut nanotubes at high reaction temperature. The length of the tube decreased with the increase of reaction time. When the temperature is low, piranha shows less damage to the nanotube surface.

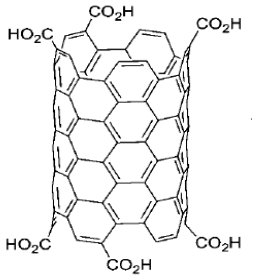

Figure 2.5 Oxidized carbon nanotube[27].

For further functionalization, the direct amino functionalization in the SWCNT opened edges was reported by Gromov and co-workers[30]. Two different pathways were shown in Figure 2.6 which demonstrate the synthesis of amino-derived SWCNTs. Amino functional group provides reactive site for further chemical/bio conjugation.

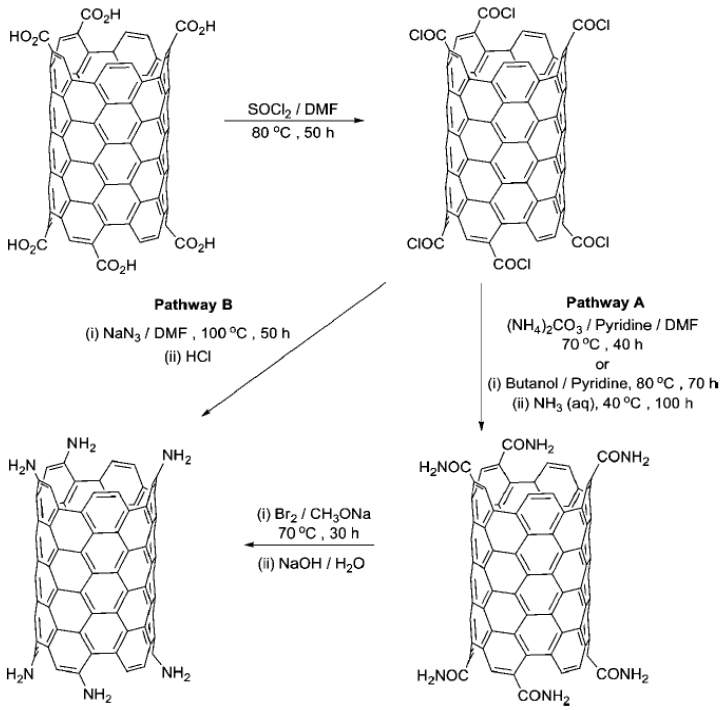

Figure 2.6 Preparation of amino-functionalized SWCNTs via Hofmann rearrangement of carboxylic acid amide (pathway A) and *via* Curtius reaction of carboxylic acid chloride with sodium azide (pathway B)[27].

For chemical functionalization on the side wall of carbon nanotubes, a widely used method is cycloaddition reaction.

Zhang, W et al. reported a cycloaddition method of carbon nanotubes using the zwitterion fragment, which is obtained by the addition of 4-aminopyridine (DMAP) and dimethylacetylene dicarboxylate (DMAD)[31]. This reaction can form a five-membered ring on the carbon nanotube sidewall (Figure 2.7). By further functionalization with an alcohol, functionalized SWCNTs can be obtained.

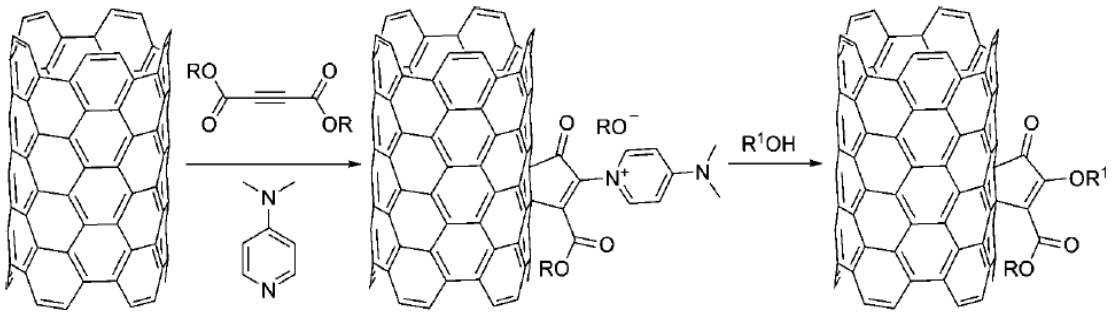

Figure 2.7 Modification of SWCNTs via dimethyl acetylenedicarboxylate-4-dimethylaminopyridine zwitterion method (R = chloroethyl, allyl, propargyl, and R^1 = methyl, dodecyl)[31].

However, even the covalent functionalization gives a stable suspension of SWCNT, this method will destroy the special chemical and covalent structure of SWCNT, significantly changing its electrical and optical property, which is necessary for optical sensing applications.

2.5.2. Non-covalent Functionalization

Surfactant suspended SWCNTs

Surfactant suspended SWCNTs was first reported by Michael J. O'Connell in 2002[33]. In this paper, the author described the method to disperse nanotubes in surfactant solution. Basically, the raw nanotube product was first added into aqueous sodium dodecyl sulfate (SDS) surfactant (1 wt %). After sonication the sample was centrifuged at 122000rpm for 4 hours. The excess surfactant was removed, only leaving the micelle-suspended nanotubes in solution. This method was the first to suspend carbon nanotubes individually in solution. This is also the first time that the bright near-infrared spectrum of SWCNTs has been observed. It is also quite interesting that when poly(vinylpyrrolidone) (PVP) was added into solution to competitive wrapping with SDS, the absorbance wavelength of the sample was red-shifted and broadened. The author described this as a result of a more polarizable and inhomogeneous environment. At

the same time, the author simulated the distribution of the SDS on the surface of SWCNTs and the solution. The result was shown in Figure 2.8.

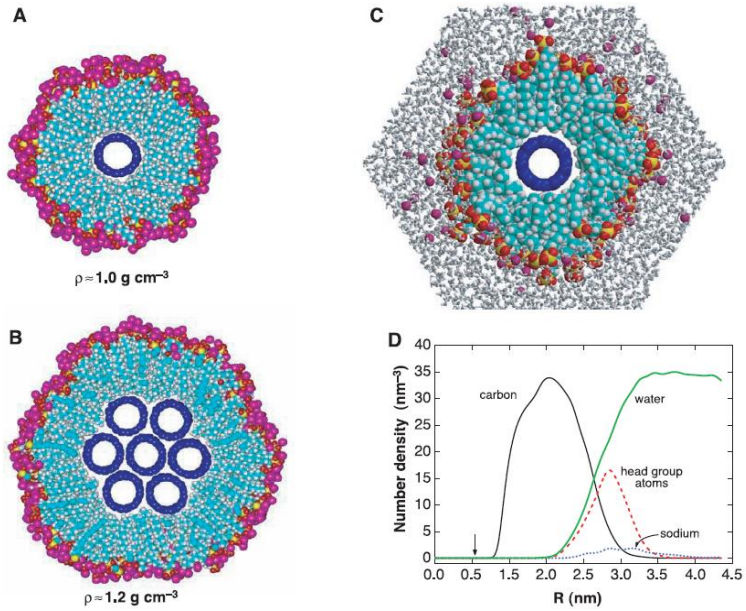

Figure 2.8 Cross-section model of (A) an individual nanotube enveloped by cylindrical SDS micelle. (B) a seven-tube bundle of nanotubes covered by SDS molecules. (C) scheme of nanotube in a water-free hydrocarbon environment. (D) The number density of carbon atoms, water molecules, sulfate head group atoms, and sodium ions[33].

Currently, numerous surfactants have been tested to suspend SWCNTs successfully, including sodium dodecylbenzenesulfonate (NaDDBS, $C_{12}H_{25}C_6H_4SO_3Na$), sodium octylbenzene sulfonate (NaOBS, $C_8H_{17}C_6H4SO_3Na$), sodium butyl benzene sulfonate (NaBBS, $C_4H_9C_6H_4SO_3Na$), sodium benzoate ($C_6H_5CO_2Na$), sodium dodecyl sulfate (SDS, $CH_3(CH_2)_{11}$-OSO_3Na), and Triton X-100[33].

However, even though surfactant can suspend SWCNTs successfully, it is not a proper choice for application in biosensor[28]. First, surfactant suspended SWCNTs only stable in excess of surfactant monomer, and it is critical to maintain the micelle of surfactant on nanotube, which is unstable. The SWCNT will aggregate again if the arrangement of the surfactant around the

carbon nanotubes is destroyed. Also, this kind of SWCNTs lacks specificity and selectivity toward analysis. Biosensors need to be worked in a complex environment and that may affect the balance of surfactant suspended SWCNTs solution. But surfactant suspended SWCNTs furthers our understanding of this special material.

Aromatic Small-Molecule suspended SWCNTs

Aromatic small molecules have also been proven to disperse carbon nanotubes[32]. Different from surfactant, aromatic molecules bind with individual SWCNTs by π-π interactions with graphitic side walls of SWCNTs[34]. It has been found that N-succinimidyl-1-pyrenebutanoate can bind to the surface of SWCNTs by π-π stacking in either *N*,*N*-dimethylformamide (DMF) or MeOH solvents[32]. These succinimidyl ester groups are reactive to proteins, for example, ferritin, by reacting with primary and secondary amines. This functionalized carbon nanotube can be used as a type of biological probe for the specific detection of different biomarkers[32].

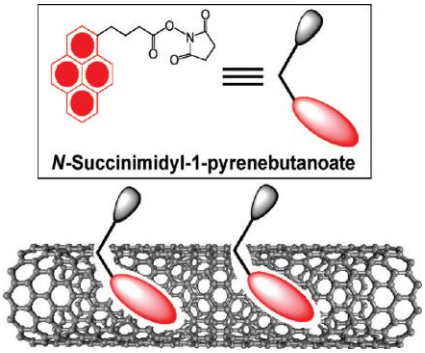

Figure 2.9 Schematic representation of N-succinimidyl-1- pyrenebutanoate-SWCNT[32].

Polymer suspended SWCNTs

Michael J. O'Connell et al. successfully dispersed nanotubes with polyvinyl pyrrolidone (PVP) and polystyrene sulfonate (PSS)[35]. In addition, they reported the mechanism of how ionic polymers suspend nanotubes. Water-soluble ionic polymer -PSS has multiple hydrophobic side

groups with a hydrophilic, linear carbon-carbon chain. The authors found that polymers can be uniformly and tightly wrapped along the surface of a nanotube and can be considered as a single entity. The polymer-SWCNTs complexes were stable for several months and can be dissolved back into solution after filtrating out if the SWCNT solution is dried. However, a high ionic strength will cause aggregation due to electric double-layer solubilization. They also presented a model to explain how this multi-helical wrapping looks like (Figure 2.10).

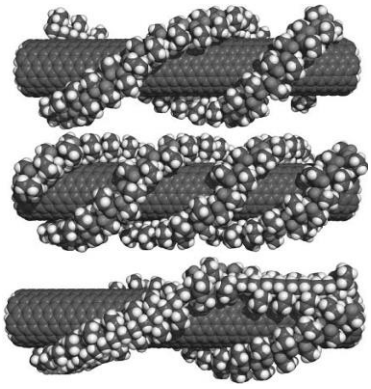

Figure 2.10 Possible wrapping construction of PVP on an (8,8) SWCNT. Double helix, triple helix or multi-layer wrapping by one polymer chain[35].

Zhuang Liu et al. developed systematic protocols for SWCNT functionalization and bioconjugation in the past few years[28]. In this protocol, Raw SWCNTs are non-covalently functionalized with phospholipid-polyethylene glycol (PL-PEG) (Figure 2.11) or other amphiphilic polymers. Functionalized SWCNTs can be dispersed in the aqueous solution. These SWCNTs can be further functionalized by reacting with specific ligands such as antibodies to enable for biological detection. In addition, these SWCNTs can be used for drug delivery as well. For instance, the authors demonstrated doxorubicin (an anticancer drug) loaded onto functionalized SWCNTs for delivery.

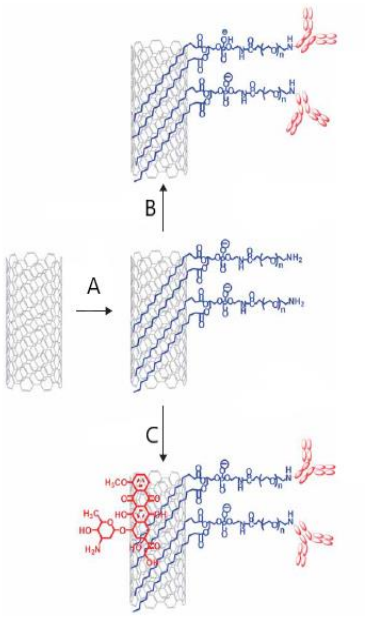

Figure 2.11 SWCNT is functionalized with phospholipid-polyethylene glycol (PL-PEG). A is the functionalization of SWNTs. B is the conjugation of targeting ligands (such as antibody) to SWCNTs. C is the loading of doxorubicin onto functionalized SWCNTs[28].

Biomolecules suspended SWCNTs

DNA-suspended SWCNTs were first reported by Ming Zheng et al[36]. They found that almost any ssDNA can disperse purified HiPco nanotubes with a denaturant after mild sonication. The effect of denaturant is to disrupt base pairing (G(guanine):C(cytosine) and A(adenine):T(thymine)) in the sequence. These disrupted bases from DNA can bind to the graphitic surface of SWCNT through π-π stacking. The fluorescence and absorption showed that SWCNTs are effectively debundled by single-stranded DNA in aqueous solution. Compared to other polymers, DNA-SWCNTs are more thoroughly dispersed, and generate helical wrapping on the surface of SWCNTs[37]. The author reported that 1 mg of DNA can disperse a same amount of HiPCO SWCNT in 1 ml solution, obtaining 0.2 to 0.4 mg/mL SWCNT solution. As an

important biomarker, DNA plays central roles in biology and could be used as a probe in biomedical applications.

2.6. SWCNT as an Optical Sensor

DNA detection

DNA detection has important implications in medicine, biology and microbiology, and has a wide range of applications in disease diagnosis[38]. Early research found that DNA can directly disperse and separate SWCNT in solution[39]. This DNA-wrapped SWCNT has been proven to detect complementary DNA sequences and single nucleotide polymorphism (SNPs) directly[39]. Due to the nano-size of SWCNT, it can be used to screen SNPs in a high throughput manner.

Detection of DNA hybridization is one of the earliest studies of SWCNT probes. Esther S. Jeng et al. using a novel method to prepare DNA-wrapped SWCNT (Figure 2.12)[38]: Cholate suspended SWCNT and DNA (5′-TAG CTA TGG AAT TCC TCG TAG GCA-3′) was added and DNA was wrapped on SWCNT by dialysis against standard Tris buffer. The combination of DNA-Wrapped SWCNT with complementary 24-mer oligonucleotide leads to a hypsochromic shift of 2meV (Figure 2.13). The detection limitation of the concentration of complementary DNA strands is 6nM. The authors built a model to demonstrate the interaction between DNA and SWCNT and they attributed the hypsochromic shift to an increased coverage of DNA on the surface of SWCNT. The kinetics showed that the hybridization of the free DNA strand was very fast (less than 10mins) while the SWCNT-bound DNA strand was slow, completing after 13h at 25℃.

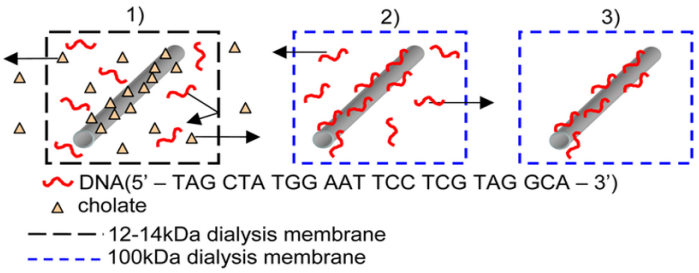

Figure 2.12 Synthesis of DNA-SWCNT[38]

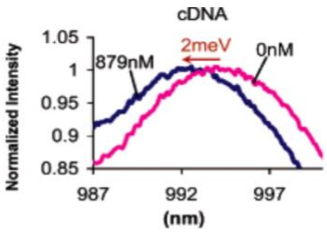

Figure 2.13 (6,5) SWCNT fluorescence change after addition of complementary DNA[38].

As significant biomarkers, MicroRNAs and other small oligonucleotides real-time detection has attracted lots of attention. Recent research has reported an engineered carbon-nanotube-based sensor for detection of hybridization of microRNA *in vivo* (Figure 2.14)[15]. A special nanotube-binding sequence was designed and reacted with a micro-capture sequence. This designed sequence was wrapped on the surface of SWCNT after sonication and centrifugation. The capture sequence can "raised up" and detach from the surface of SWCNT in the presence of target microRNA, resulting in the competitive effects between displacement of both oligonucleotide charge groups and water from the nanotube surface, which will cause the fluorescence change and wavelength shift of SWCNT solution. These competitive effects changed the dielectric and electrostatic factors in the local environment around nanotubes and thus changed the photoluminescence. Based on this, the authors added amphiphilic moieties

(SDBS) in samples which can replace water molecules on the surface of carbon nanotubes, resulting in a markedly enhanced spectral response. By using different SWCNT chiralities, this sensor was proven to enable multiplexed detection. The encasing of sensors in an implantable device and the detection of target microRNA for live mice was also illustrated.

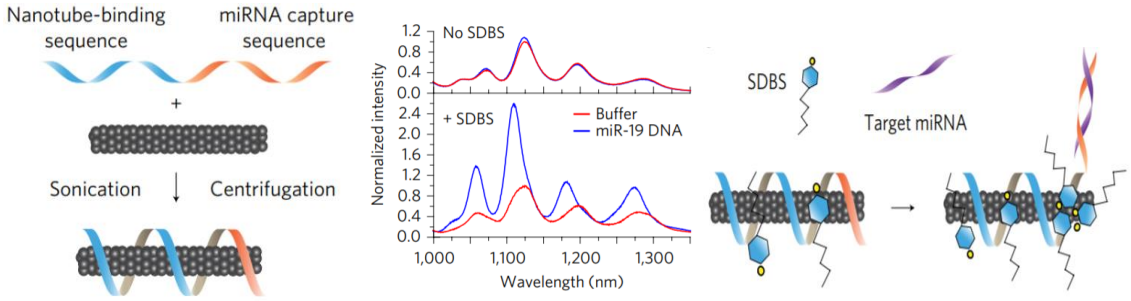

Figure 2.14 Mechanism of SWCNT sensor for miRNA. (a) Construction of the miRNA sensor complex. (b) Fluorescence of nanotube sensors with miR-19 DNA and SDBS. (c) Mechanism of SDBS-mediated enhancement of the blue-shift response to hybridization[15].

Protein and other Biomarkers detection

Protein biomarkers refer to a class of proteins that can aid diagnosis[26]. The requirement of biomarkers detection is fast, sensitive and accurate. Currently nanomaterial has attracted a lot of attention because it allows label free detection, which allows direct analysis of target biomarkers without secondary steps[26]. SWCNT is a desired material for label free detection because of its special optical properties. The design of a biomarker SWCNT optical sensor has the following steps: The synthesis of reactant for target biomarker, the combination of SWCNT and reactant and the analyzing of fluorescence spectroscopy of complex[26].

Microalbuminuria has been proven to be a significant biomarker for several diseases[40]. However, the label-based method required several steps and was not suitable for real-time detection. Polycarbodiimide-SWCNT (PCD-SWCNT) complexes were synthesized for label free

detection of albumin[40]. Polymer with phenyl rings and carboxyl functional group showed a hypsochromic (blue) shift and fluorescence intensity enhancement in the presence of albumin protein (Figure 2.15). The sensor was found sensitive and specific for albumin detection in clinical samples. This sensor was combined with acrylic material to prepare a solid-state nano-sensor paint albumin sensor that can be applied to point-of-care detection.

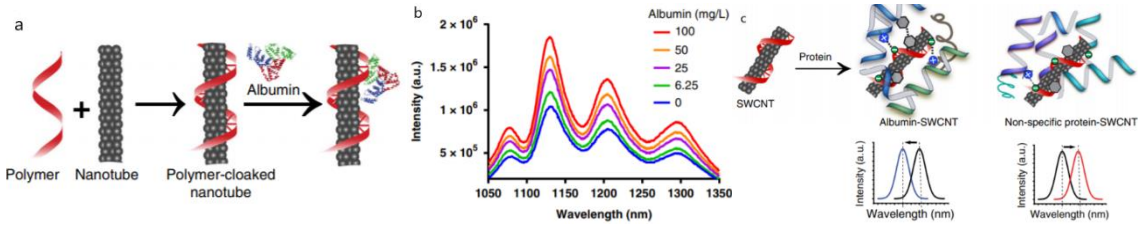

Figure 2.15 SWCNT sensor for albumin detection (a) Construction of PCD-SWCNT complex. (b) Fluorescence spectra of carboxy-PCD-SWCNT after addition of albumin. (c) albumin interaction with the carboxy-PCD-SWCNT[40].

Serotonin is a neurotransmitter produced in the body and exists in some plants and fungi. Serotonin can affect people's appetite, internal drive (appetite, sleep, sex) and mood[41]. Meshkat Dinarvand et al. designed a SWCNT optical sensor for serotonin with a serotonin binding DNA aptamer combined on the surface of SWCNT (Figure 2.16)[41]. It showed a fluorescence intensity enhancement in the presence of serotonin by a factor up to 1.8 and generated a dynamic linear range of detection from 100nM to 1μM in the physiologically relevant region. Compared with traditional methods, this approach can obtain spatial information (on single cell level) and the amount of data (multiple cells at the same time), demonstrating the strong potential of carbon nanotubes in biomedical applications.

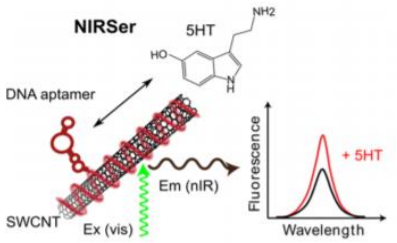

Figure 2.16 Interaction of Serotonin (5HT) with serotonin nano-sensor NIRSer[41].

Ahn et al. reported a novel method using SWCNT to achieve protein detection in the analysis of protein-protein interactions[42]. In this approach, chitosan polymer was modified with nitrilotriacetic acid (NTA) and wrapped around SWCNT. After chelating with Ni^{2+}, the NTA-Ni^{2+} could work as a quencher and change the fluorescence intensity based on the distance of ion and SWCNT. This complex can bind to any captured protein with a hexahistidine tagged (His-tag). This binding process will decrease the distance of the ion from SWCNT. Upon the binding with analyte protein the distance was changed and caused fluorescence intensity changes, either increasing or decreasing at different levels. This approach allowed detection in a single protein level at a complicated environment.

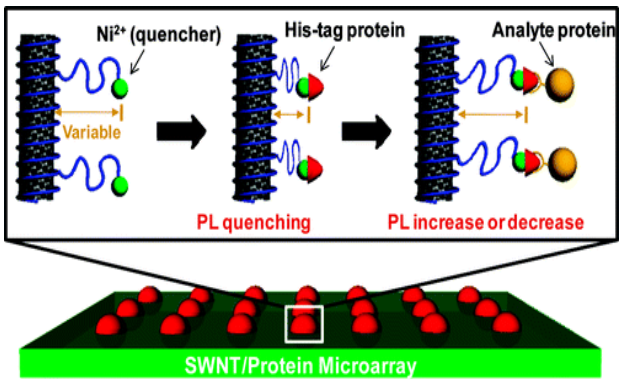

Figure 2.17 Construction and mechanism of SWCNT/protein microarray[42].

Daniel P. Salem et al. reported an SWCNT-based sensor platform[43] using Protein A (rPA, His-tagged at N-terminus) functionalized SWCNT and coupled with a hydrogel matrix. This sensor can achieve rapid detection of IgG1 aggregation. The authors demonstrated the control of hydrogel matrix to the protein diffusion.

Doxorubicin is an FDA approved anticancer therapy that has the strongest inhibitory effects on RNA. However, it has intractable dose-limiting toxicities, and the detection in preclinical measurement remains problems[44]. Jackson D. Harvey et al. provided a SWCNT optical sensor for detection of doxorubicin in living organisms[44]. The authors found that the SWCNT functionalized by DNA showed a large and uniform red-shift in the presence of DNA-intercalating agents, including anthracycline compounds such as doxorubicin (Figure 2.18). These DNA-SWCNTs showed irreversible red shifting based on the concentration of doxorubicin between 500 nM and 50 μM. This sensor was incorporated into an implantable membrane and succeeded in real-time, minimally invasive monitoring of doxorubicin in the peritoneal cavity.

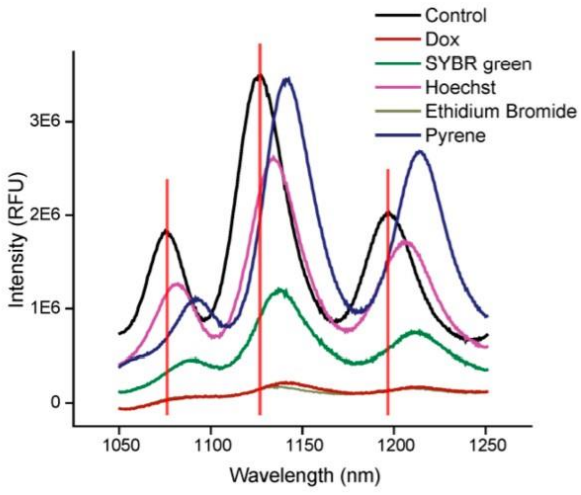

Figure 2.18 Photoluminescence spectra of DNA-SWCNT nanosensors upon addition of DNA-intercalating agents[45].

Hong et al. used SWCNT for detection of H_2O_2[45]. An array of fluorescent single-walled carbon nanotubes was built by suspending SWCNT in type I collagen. The fluorescence was found to be step quenched after addition of H_2O_2. It was found that the signal of epidermal growth factor receptor (EGFR), which is over-expressed by A431 cells, was captured by this array successfully. Recently, a HeAptDNA-SWCNT was reported to detect H_2O_2 in plants to monitor plant health[46]. It has been found that plants are likely to generate H_2O_2 in response to stress reactions. The fluorescence of HeAptDNA-SWCNT quenches upon the absorption of H_2O_2 and the differences in fluorescence quenching and recovery open opportunities for modeling stress levels and patterns.

A recent research[47] used sodium cholate to disperse carbon nanotubes, and explored its optical response to neurotransmitters, amino acids, and sugars. By adjusting the concentration of the surfactant in the carbon nanotube solution to be lower than the critical micelle concentration, the exposed area of the carbon nanotube is increased. This made the sodium cholate-carbon nanotubes selective for serotonin.

Daniel P. Salem et al. successfully immobilized SWCNTs onto paper substrates while maintaining a high sensitivity[48] towards metal ion detection. The sensor comprised of ssDNA-wrapped SWCNTs had the ability to distinguish metal ions such as Cu(II), Cd(II), Hg(II), and Pb(II) at a concentration of 100 μM.

2.7 Protamine and Its Detection

Protamine is a low molecular weight protein rich in arginine residues, which gives it a great quantity of positive charges[49]. In the medical field, the major application of protamine is to inhibit the release of insulin[50] and serve as antagonist for heparin, particularly to prevent the coagulation caused by overdose of heparin during cardiac surgery[52]. Due to the highly positive

charges, protamine can bind heparin through electrostatic interactions. Protamine also can be used to reduce platelet in blood vessels and be used to enhance fibrinolysis[52]. It was originally isolated from salmon fish and now mostly made by recombinant biotechnology[52].

Applications of protamine

The application of protamine as a drug can be traced back to the 1930s. Protamine was obtained from the sperm of California rainbow trout and used it to prolong the effect of neutral protamine insulin to assist in the treatment of diabetes[52]. For a long time afterwards, protamine was widely used as a neutralizing agent for heparin in surgical operations. It has been proved that protamine can effectively reduce the complications caused by stent implantation such as transient back pain, hypotension, and skin rashes were well managed in vitro, and reduce the length of hospital stay[49]. Recently, Tadao Fukushima et al. reported the application of protamine in dental medicine. The authors synthesized a DNA/protamine complex paste and proved that it has bacteriostatic effect when injected as a dental implant[50]. A study found that heparin and protamine can promote blood vessel production and cell regeneration. The study used a mice model and observed a significant increase in the rate of angiogenesis and tissue formation after Fragmin/Protamine injection. Meanwhile, the application of protamine in tissue engineering and drug delivery has attracted a lot of attention[51].

Detection of protamine

Despite the wide range of medical uses of protamine, plenty of side effects had been reported. For example, it may lead to systemic hypotension, anaphylactic reactions, and pulmonary vasoconstriction with secondary right heart failure[52 55]. Hence, it is necessary to design a convenient and efficient method to detect the concentration of protamine. Currently, there are several methods for quality measurement of protamine, such as chromatographic

method[55], high-performance liquid chromatography[56], electrochemical analysis[58]and antibody test[59].

Enju Wang et al. reported a method for detection of protamine using optical films[56]. The authors synthesized a Lipophilic 2 ,7 -dichlorofluorescein esters and incorporated it into a membrane film. This optical film can absorb protamine by a cation exchange of protamine and proton. This exchange will cause the change of absorbance of polymeric film and thus can be used as a protamine sensor. This optical film has high selectivity for protamine in blood and is a response to micro molar level.

High-performance liquid chromatography can be used for detection of protamine[53]. David Awotwe-Otoo et al. reported a robust reverse phase-HPLC method for quality detection of protamine. This method can separate protamine sulfate into its four peptide peaks with high chromatographically efficiency.

Yibing Liu et al. designed a n MPA-AgInZnS quantum dots (AIZS QDs) for detection of protamine and trypsin (Figure 2.19)[57]. The interaction between AIZS QDs and protamine will cause the aggregation of QDs and thus increase the fluorescence intensity (Figure 2.20). Trypsin worked as a decomposition of protamine and led to the decreasing fluorescence intensity of AIZS QDs/protamine complexes. This nanosensor is cost-effective and convenient compared to other methods.

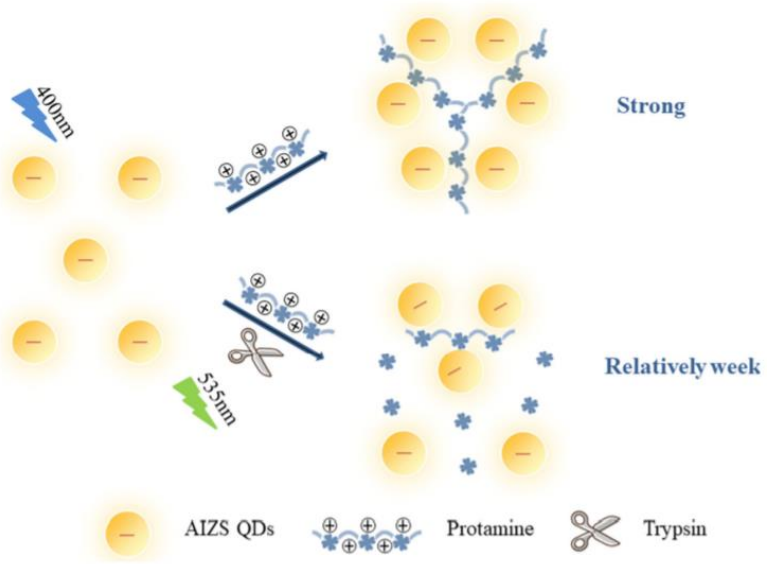

Figure 2.19 Detection of protamine and trypsin by MPA-AgInZnS quantum[57].

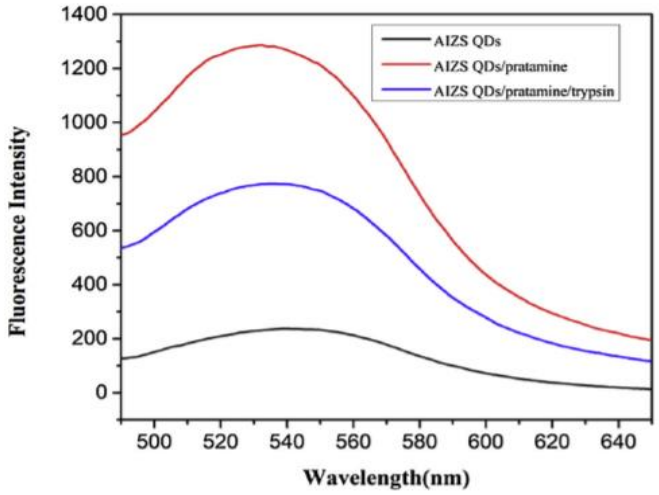

Figure 2.20 Photoluminescence spectra of AIZS QDs, AIZS QDs/protamine (50 μg mL^{-1}), AIZS QDs/protamine (50 μg mL^{-1}) /trypsin (3.0 μg mL^{-1})[57].

However, some of these methods such as antibody test and high-performance liquid chromatography are hard to operate or time-consuming. To facilitate accurate detection, we provided a protamine nano-sensor based on the SWCNT platform in this study.

CHAPTER 3

EXPERIMENTAL METHOD AND MATERIAL

3.1. Experimental Method and Materials

Material: Sodium Cholate (SC), sodium dodecyl sulfate (SDS), sodium dodecanoate (Also called sodium laurate), sodium dodecylbenzenesulfonate (SDBS), poly(sodium 4-styrenesulfonate) (PSS), poly(diallyldimethylammonium chloride) (PDADMAC), poly(allylamine hydrochloride) (PAH) Poly acrylic acid (PAA), PBS buffer and protamine were obtained from Sigma-Aldrich. Two different SWCNTs were used: (7,6) SWCNT (Aldrich, product code 1002641539) and (6,5) SWCNT (ALDRICH, Product number 1002931991).

General method: SWCNT suspensions were made at 1 mg of SWCNT/mL of water. All the surfactant-SWCNT systems were made at 1 mg/mL SWCNT in a 2% (by wt.) surfactant solution. A typical suspension volume of 1 mL in a 1.5 mL tube was used for all experiments. Sonicator was used for 15mins at 20% AMP for each sample, with the tube in a CoolRack immersed in ice. The suspension may be sonicated longer until no obvious black solid part in solution. Suspensions that appeared stable and no obvious precipitation after sonication, were centrifuged at 14000rpm for 30mins. The supernatant was taken out after first centrifugation and centrifuged again at 14000rpm for 30mins. The resulting supernatant was used for further measurements. A typical condition, 3000ms integration, 3 averaging, for fluorescence was used for all measurements. The fluorescence intensity is obtained from the spectral data in the interval of 950nm-1200nm wavelength. For PSS-SWCNTs, UV-vis-NIR spectra of stable suspensions were recorded for the calculation of the concentration of SWCNT. The concentration of stable SWCNT suspensions was determined from optical absorption spectroscopy using the Beer-

Lambert law: A=alc. A is the absorbance, a is the extinction coefficient, l is the path length, and c is the concentration.

Instrument: Sonicator (FB505110, Fisherbran Model 505 Sonic Dismembrator), Centrifuge (75002436, Thermo Scientific™ Sorvall™ Legend™ Micro 21 Microcentrifuge), NS-MiniTracer (NanoSpectralyzer from Applied NanoFluorescence). UV-vis-NIR (Cary 5000 from Agilent).

3.2. Fluorescence measurement of surfactant-SWCNT systems

3.2.1. Preparation of sodium cholate (SC)-(7,6) SWCNT and fluorescence measurement

A 2% SC solution was prepared by weighing out 0.2g SC and adding into 10mL DI-water. 1 mg of (7,6) SWCNTs was added to 1 mL of 2% SC solution in a microcentrifuge tube (1.5 mL). The mixture of SC and (7,6)-enriched SWCNT was sonicated for 30 mins (AMP 20%) at low temperature using a CoolRack (precooled at -20 °C and with ice around). After sonication, the sample was centrifuged for 30mins, 14000 RPM at room temperature. Upon centrifugation, the supernatant was collected and re-centrifuged under the same conditions. The supernatant was then collected and diluted in water as required (5, 10, 20 folds dilution) to obtain SC-(7,6) SWCNT solution. Near infra-red fluorescence of the dilute SC-(7,6) SWCNT solutions were measured.

3.2.2. Preparation of sodium cholate (SC)-(6,5) SWCNT and fluorescence measurement

A 2% SC solution was prepared by weighing out 0.2g SC and adding into 10ml DI-water. 1 mg of (6,5) SWCNTs was added to 1 mL of 2% SC solution in a microcentrifuge tube (1.5ml). The mixture of SC and (6,5)-enriched SWCNT was sonicated for 30mins (AMP 20%) at low temperature using a CoolRack (precooled at -20°C and with ice around). After sonication, the sample was centrifuged for 30mins, 14000RPM at room temperature. Upon centrifugation, the

supernatant was collected and re-centrifuged under the same condition. The supernatant was then collected and diluted in water as required (5, 10 folds) to obtain SC-(6,5) SWCNT solution. Near infra-red fluorescence of the dilute SC-(6,5) SWCNT solutions were measured.

3.2.3. Preparation of sodium dodecyl sulfate (SDS)-(7,6) SWCNT and fluorescence measurement

A 2% SDS solution was prepared by weighing out 0.2g SDS and adding into 10ml DI-water. 1 mg of (7,6) SWCNTs was added to 1 mL of 2% SDS solution in a microcentrifuge tube (1.5 mL). The mixture of SDS and (7,6)-enriched SWCNT was sonicated for 30 mins (AMP 20%) at low temperature using a CoolRack (precooled at -20 °C and with ice around). After sonication, the sample was centrifuged for 30mins, 14000 RPM at room temperature. Upon centrifugation, the supernatant was collected and re-centrifuged under the same conditions. The supernatant was then collected and diluted in water as required (5, 10, 20 folds) to obtain SDS -(7,6) SWCNT solution. Near infra-red fluorescence of the dilute SDS-(7,6) SWCNT solutions were measured.

3.2.4. Preparation of sodium dodecyl sulfate (SDS)-(6,5) SWCNT and fluorescence measurement

A 2% SDS solution was prepared by weighing out 0.2g SDS and adding into 10ml DI-water. 1 mg of (6,5) SWCNTs was added to 1 mL of 2% SDS solution in a microcentrifuge tube (1.5 mL). The mixture of SDS and (6,5)-enriched SWCNT was sonicated for 30 mins (AMP 20%) at low temperature using a CoolRack (precooled at -20 °C and with ice around). After sonication, the sample was centrifuged for 30mins, 14000 RPM at room temperature. Upon centrifugation, the supernatant was collected and re-centrifuged under the same conditions. The supernatant was then collected and diluted in water as required (5, 10, 20 folds) to obtain SDS -

(6,5) SWCNT solution. Near infra-red fluorescence of the dilute SDS-(6,5) SWCNT solutions were measured.

3.2.5. Preparation of sodium dodecylbenzenesulfonate (SDBS)-(7,6) SWCNT and fluorescence measurement

A 2% SDBS solution was prepared by weighing out 0.2g SDBS and adding into 10ml DI-water. 1 mg of (7,6) SWCNTs was added to 1 mL of 2% SDBS solution in a microcentrifuge tube (1.5 mL). The mixture of SDBS and (7,6)-enriched SWCNT was sonicated for 30 mins (AMP 20%) at low temperature using a CoolRack (precooled at -20 °C and with ice around). After sonication, the sample was centrifuged for 30mins, 14000 RPM at room temperature. Upon centrifugation, the supernatant was collected and re-centrifuged under the same conditions. The supernatant was then collected and diluted in water as required (5, 10, 20 folds) to obtain SDBS -(7,6) SWCNT solution. Near infra-red fluorescence of the dilute SDBS-(7,6) SWCNT solutions were measured.

3.2.6. Preparation of Sodium laurate -(7,6) SWCNT and fluorescence measurement

A 2% sodium laurate solution was prepared by weighing out 0.2g sodium laurate and adding into 10ml DI-water. 1 mg of (7,6) SWCNTs was added to 1 mL of 2% sodium laurate solution in a microcentrifuge tube (1.5 mL). The mixture of sodium laurate and (7,6)-enriched SWCNT was sonicated for 30 mins (AMP 20%) at low temperature using a CoolRack (precooled at -20 °C and with ice around). After sonication, the sample was centrifuged for 30mins, 14000 RPM at room temperature. Upon centrifugation, the supernatant was collected and re-centrifuged under the same conditions. The supernatant was then collected and diluted in water as required (5, 10, 20 folds) to obtain sodium laurate-(7,6) SWCNT solution. Near infra-red fluorescence of the dilute sodium laurate-(7,6) SWCNT solutions were measured.

3.3. Effect of poly(diallyldimethylammonium chloride) (PDADMAC) on surfactant-SWCNT systems

A 2% PDADMAC solution was prepared by diluting 20% PDADMAC solution in DI water. All experiments in this section were performed in triplicate.

3.3.1. Effect of PDADMAC on SC- (7,6) SWCNT

100µl of 2% PDADMAC solution was added into 400µL of 5-folds diluted SC- (7,6) SWCNT and the solution was mixed thoroughly. For the control sample, 100µL water was added to 400µL 5-folds diluted SC- (7,6) SWCNT. The near infra-red fluorescence was measured for each sample.

3.3.2. Effect of PDADMAC on SC- (6,5) SWCNT

For SC-(6,5) SWCNT solution, the same procedure was used to run experiments and collect data.

3.3.3. Effect of PDADMAC on SDS- (7,6) SWCNT

100µL of 2% PDADMAC solution was added into 400µL of 5-folds diluted SDS- (7,6) SWCNT and the solution was mixed thoroughly. For the control group, 100µL water was added to 400µL of 5-folds diluted SDS- (7,6) SWCNT. The near infra-red fluorescence was measured for each sample.

3.3.4. Effect of PDADMAC on SDS- (6,5) SWCNT

100µL of 2% PDADMAC solution was added into 400µL of 5-folds diluted SDS- (6,5) SWCNT and the solution was mixed thoroughly. For the control group, 100µL water was added to 400µL of 5-folds diluted SDS- (6,5) SWCNT. The near infra-red fluorescence was measured for each sample.

3.3.5. Effect of PDADMAC on SDBS- (7,6) SWCNT

100μL of 2% PDADMAC solution was added into 400μL of 5-folds diluted SDBS- (7,6) SWCNT and the solution was mixed thoroughly. For the control group, 100μL water was added to 400μL of 5-folds diluted SDBS- (7,6) SWCNT. The near infra-red fluorescence was measured for each sample.

3.3.6. Effect of PDADMAC on sodium laurate- (7,6) SWCNT

100μL of 2% PDADMAC solution was added into 400μL of 5-folds diluted sodium laurate- (7,6) SWCNT and the solution was mixed thoroughly. For the control group, 100μL water was added to 400μL of 5-folds diluted sodium laurate- (7,6) SWCNT. The near infra-red fluorescence was measured for each sample.

3.4. Effect of poly(allylamine hydrochloride) (PAH) on surfactant-SWCNT systems

2% PAH solution was prepared by weighing out 0.2g PAH and adding into 10ml DI-water. All experiments in this section were performed in triplicate.

3.4.1. Effect of PAH on SC- (7,6) SWCNT

100μL of 2% PAH solution was added into 400μL of 5-folds diluted SC- (7,6) SWCNT and the solution was mixed thoroughly. For the control group, 100μL water was added to 400μL of 5-folds diluted SC- (7,6) SWCNT. The near infra-red fluorescence was measured for each sample.

3.4.2. Effect of PAH on SC- (6,5) SWCNT

100μL of 2% PAH solution was added into 400μL of 5-folds diluted SC- (6,5) SWCNT and the solution was mixed thoroughly. For the control group, 100μL water was added to 400μL of 5-folds diluted SC- (6,5) SWCNT. The near infra-red fluorescence was measured for each sample.

3.4.3. Effect of PAH on SDS- (7,6) SWCNT

100μL of 2% PAH solution was added into 400μL of 5-folds diluted SDS- (7,6) SWCNT and the solution was mixed thoroughly. For the control group, 100μL water was added to 400μL of 5-folds diluted SDS- (7,6) SWCNT. The near infra-red fluorescence was measured for each sample.

3.4.4. Effect of PAH on SDS- (6,5) SWCNT

100μL of 2% PAH solution was added into 400μL of 5-folds diluted SDS- (6,5) SWCNT and the solution was mixed thoroughly. For the control group, 100μL water was added to 400μL of 5-folds diluted SDS- (6,5) SWCNT. The near infra-red fluorescence was measured for each sample.

3.4.5. Effect of PAH on SDBS- (7,6) SWCNT

100μL of 2% PAH solution was added into 400μL of 5-folds diluted SDBS- (7,6) SWCNT and the solution was mixed thoroughly. For the control group, 100μL water was added to 400μL of 5-folds diluted SDBS- (7,6) SWCNT. The near infra-red fluorescence was measured for each sample.

3.4.6. Effect of PAH on sodium laurate- (7,6) SWCNT

100μL of 2% PAH solution was added into 400μL of 5-folds diluted sodium laurate- (7,6) SWCNT and the solution was mixed thoroughly. For the control group, 100μL water was added to 400μL of 5-folds diluted sodium laurate- (7,6) SWCNT. The near infra-red fluorescence was measured for each sample.

3.5. Effect of poly acrylic acid (PAA) on surfactant-SWCNT systems

A 2% PAA solution was prepared by weighing out 0.2g PAA and adding into 10ml DI-water. All experiments in this section were performed in triplicate.

3.5.1. Effect of PAA on SDBS-(7,6) SWCNT

100μL of 2% PAA solution was added into 400μL of 5-folds diluted SDBS- (7,6) SWCNT and the solution was mixed thoroughly. For the control group, 100μL water was added to 400μL of 5-folds diluted SDBS- (7,6) SWCNT. The near infra-red fluorescence was measured for each sample.

3.5.2. Effect of PAA on sodium laurate-(7,6) SWCNT

100μL of 2% PAH solution was added into 400μL of 5-folds diluted sodium laurate-(7,6) SWCNT and the solution was mixed thoroughly. For the control group, 100μL water was added to 400μL of 5-folds diluted sodium laurate- (7,6) SWCNT. The near infra-red fluorescence was measured for each sample.

3.6. Preparation of PSS-SWCNT

PSS solution was prepared by weighing out 5mg PSS and adding into 1ml DI-water. 1 mg (6,5) of SWCNTs was added to 1 mL of PSS solution. The mixture of PSS and (6,5)-enriched SWCNT was placed on CoolRack (precooled at -20 °C) with ice around and sonicated for 15 mins, AMP 20%. After sonication, the sample was centrifuged for 15mins, 14000RPM at room temperature. Upon centrifugation, the supernatant was collected, and the sample was sonicated again in the same condition for a few seconds. Then the sample was centrifuged for 30mins, 14000RPM at room temperature. The supernatant was taken out and centrifuged again for 30mins, 14000RPM. After the third centrifuge, the supernatant was taken to obtain the PSS-(6,5) SWCNT solution. The stock nanotube solution was diluted 10-folds in water and used for

the experiments. The concentration of PSS- (6,5) SWCNT was solution was determined via UV-Vis-NIR absorbance spectroscopy.

3.6.1. Effect of PDADMAC on PSS-(6,5) SWCNT

100μL of 2% PDADMAC solution was added into 300μL of 10-folds diluted PSS- (6,5) SWCNT. The solution was mixed thoroughly. For the control group, 100μL water was added to 300μL PSS- (6,5) SWCNT. The fluorescence was measured for each sample.

3.6.2. Effect of PAH on PSS-(6,5) SWCNT

100μL of 2% PAH solution was added into 300μL of 10-folds diluted PSS- (6,5) SWCNT. The solution was mixed thoroughly. For the control group, 100μL water was added to 300μL - (6,5) SWCNT. The fluorescence was measured for each sample.

3.6.3. Effect of protamine on PSS -(6,5) SWCNT

The optical response of different concentration of protamine to PSS- (6,5) SWCNT was measured in this section. The change in fluorescence intensity is the main focus of this experiment. A 10-folds diluted PSS- (6,5) SWCNT solution was used in the following experiments.

3.6.3.1. Protamine concentration (0-2500mg/L)

10mg/mL protamine solution (S1) was prepared in PBS solution. A 500mg/L protamine solution(S2) was prepared by diluting S1. The same method was used to obtain 400mg/L protamine solution (S3), 200mg/L protamine solution (S4). All the protamine solution was stored in the refrigerator after preparation.

80μL S1 was added into 320μL PSS- (6,5) SWCNT solution. In this experiment, we mainly focus on the concentration of protamine in PSS- (6,5) SWCNT solution. In the first sample, the final concentration of protamine in nanotube solution was 2mg/mL. Samples with

various concentration of protamine in nanotube solution were prepared by adding 100μL S1, S2, S3 and S4 was added into 300μL nanotube solution respectively. The final concentration of protamine in nanotube solution was 2500mg/L, 125mg/L, 100mg/L and 50mg/L respectively. For control sample, 100μL PBS solution was added. All samples were mixed thoroughly incubated at room temperature for 15 minutes for equilibrium prior to fluorescence measurements. This experiment was performed once due to lab closure amid COVID-19 situation.

3.6.3.2. Protamine concentration (0-1000mg/L)

The same method was used to obtain final concentration 50mg/L, 100mg/L, 200mg/L, 500mg/L and 1000mg/L protamine in nanotube solution. For control sample, 100μL PBS solution was added. All samples were mixed thoroughly and incubated at room temperature for 15 minutes for equilibrium prior to fluorescence measurements and the experiment was triplicated.

3.6.3.3. Protamine concentration (1000mg/L)

Fluorescence of eight different samples with 1000mg/L protamine in nanotube solution was measured. All the data was organized in figure 4.26.

3.6.3.4. Protamine concentration (0-30mg/L)

The same method was used to obtain final concentration 5mg/L, 10mg/L, 15mg/L, 20mg/L, 25mg/L and 30mg/L protamine in nanotube solution. For control, 100μL PBS solution was added. All samples were mixed thoroughly incubated at room temperature for 15 minutes for equilibrium prior to fluorescence measurements.

3.6.4. Kinetics experiment of PSS-(6,5) SWCNT with 50mg/L protamine

50mg/L protamine in nanotube solution was prepared. Fluorescence was measured immediately after adding the protamine solution (without mixing) and this time point was considered a starting point. Fluorescence was measured every five minutes for an hour.

3.6.5. PSS- (6,5) SWCNT with 0.02% PDADMAC, PAH and protamine solution

0.02% PDADMAC solution was prepared by diluting 2% PDADMAC solution in water and 0.02% PAH solution was prepared by diluting 2% PAH solution. 0.02% protamine solution (200mg/L) was taken from S4. 100µL 0.02% PDADMAC, 0.02% PAH and 0.02% protamine were added into 300µL PSS- (6,5) SWCNT solution. For control, 100µL water was added into 300µL PSS- (6,5) SWCNT. All samples were mixed thoroughly and incubated at room temperature for 15 minutes for equilibrium prior to fluorescence measurements.

3.6.6. PAA- (6,5) SWCNT with 0.02% PDADMAC, PAH and protamine solution

PAA- (6,5) SWCNT was prepared by using the same method as PSS-(6,5) SWCNT. 100µL 0.02% PDADMAC, 0.02% PAH and 0.02% protamine were added into 300µL PAA- (6,5) SWCNT solution. For control, 100µL water was added into 300µL PAA- (6,5) SWCNT. All samples were mixed thoroughly and incubated at room temperature for 15 minutes for equilibrium prior to fluorescence measurements.

CHAPTER 4

DATA AND DISCCUSION

4.1. Fluorescence of surfactant-SWCNT system

SC, SDS, SDBS and sodium laurate are four commonly used surfactants used to disperse single-walled carbon nanotubes (SWCNTs) in aqueous solution. In this experiment, we measured the fluorescence of (7,6)- and (6,5)-enriched SWCNTs dispersed with the aid of surfactants in aqueous solvent.

The structures of surfactants are shown in figure 4.1. The surfactants were used to disperse SWCNTs to prepare aqueous suspension using a common method. The surfactants used in these experiments are anionic and therefore, resulting surfactant-SWCNTs exhibit negative surface charge[25]. From figure 4.2 we can know that SC has the best efficient for both (7,6) and (6,5) SWCNT. Different SWCNTs have different affinities for surfactants. Qualitative analysis of these solutions and residue left (unsuspended) upon sample preparation showed that SC surfactant has the highest efficiency and SDS has the least efficiency in dispersion of SWCNTs in aqueous solvents compared to other surfactants used under similar experimental conditions. Figure 4.2 shows the fluorescence of each surfactant dispersed SWCNTs. Photoluminescence of surfactant dispersed SWCNTs has been found to vary depending on the exact surfactant used[2]. For example, SDS-SWCNTs appeared to exhibit lower photoluminescence as compared to SC-SWCNTs of similar concentration. This observation is similar with previous reports[58]. SDS-SWCNTs were also found to be less stable in solution as compared to SC-SWCNTs as determined from visual inspection of aggregation over a period of time. Interestingly, the stability of SDS-SWCNTs varied with the nature of SWCNTs. For example, suspension of SDS-(6,5) enriched SWCNTs was found more stable compared to SDS-(7,6) enriched SWCNTs

prepared under similar experimental conditions. SC and SDBS are bulky structure with carboxylic group while SDS and sodium laurate are linear alkyl structure with sulfonate group. SC and sodium laurate contain carboxylic groups whereas SDBS and SDS contain sulfonate groups. Among the surfactants employed, SC-SWCNTs exhibited a higher emission intensity. Furthermore, we observed that nanotubes suspended with surfactants comprising carboxylic groups exhibit relatively higher fluorescence intensity compared with the nanotubes dispersed in surfactants which contain sulfonate groups (Figure 4.1). This observation that the sulfonated surfactants somehow quench the fluorescence on SWCNTs as compared to carboxylated surfactants is unprecedented. Further investigation on this phenomenon is currently underway in our laboratory.

We used chirality enriched (7,6) or (6,5) SWCNTs with >90% enrichment in this experiment. (7,6)-SWCNTs and (6,5)-SWCNTs are known to exhibit emission in between 1100 nm-1150 nm, and 950 nm-1000 nm and absorption in between 600 nm-650 nm and 550 nm-600 nm respectively[13]. However, we observed an additional emission peak around 1135nm in all the solution, which could be assigned to (7,5) SWCNT, based on both emission and absorption spectra. The intensity of absorption peak showed (7,5) SWCNTs as a minor component. Photoluminescence spectra, however, showed a descent emission intensity from (7,5) SWCNT, most likely due to in-resonance excitation of (7,5) SWCNTs by 638 nm LASER used in the experiment.

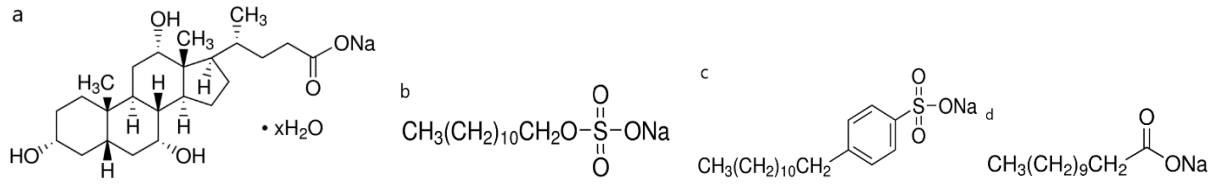

Figure 4.1 Structure of surfactants. (a) Sodium cholate. (b) Sodium dodecyl sulfate. (c) Sodium dodecylbenzenesulfonate. (d) Sodium dodecanoate/Sodium laurate.

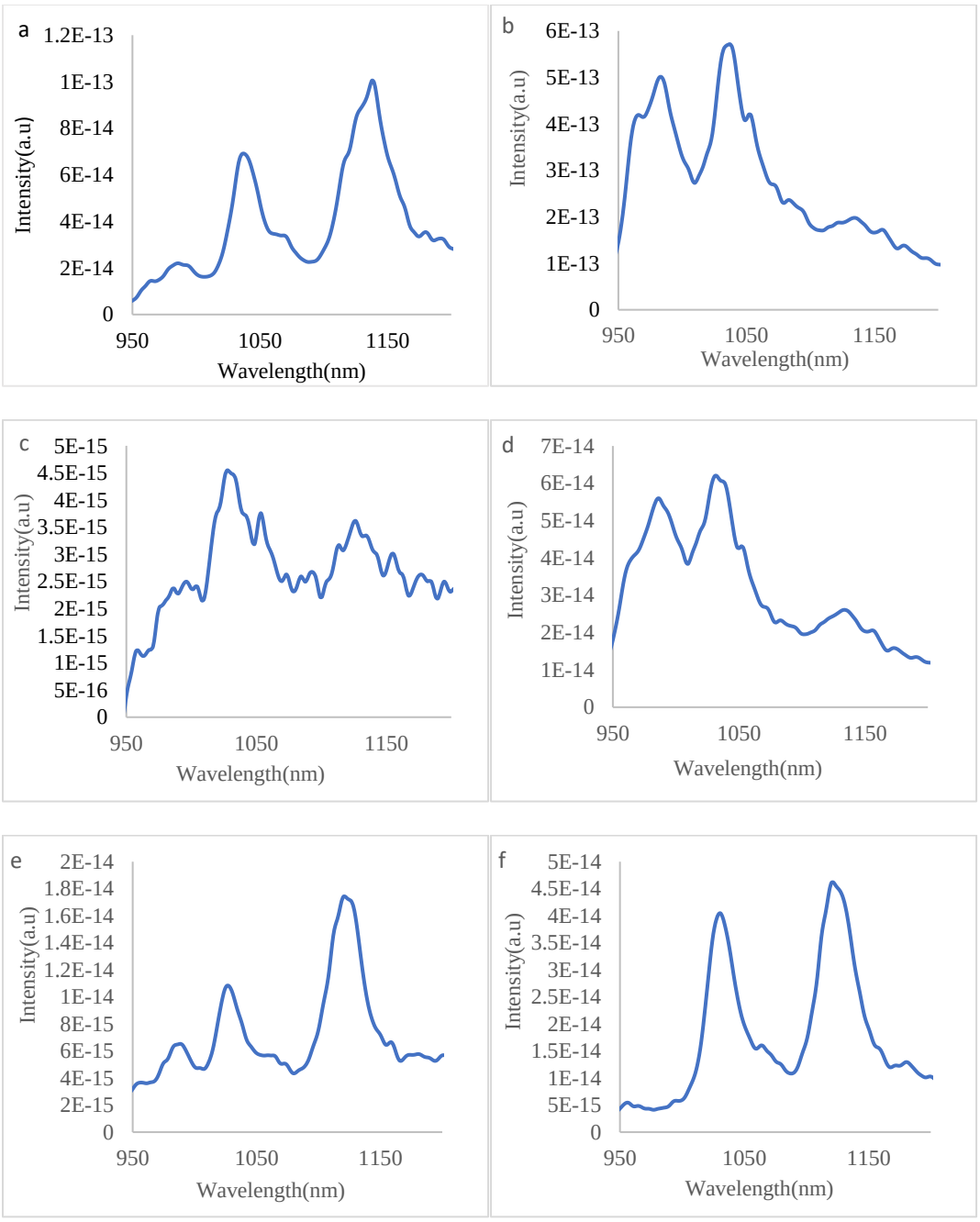

Figure 4.2 Fluorescence of (a) SC-(7,6) SWCNT, (b) SC-(6,5) SWCNT, (c) SDS-(7,6) SWCNT, (d) SDS-(6,5) SWCNT, (e)SDBS-(7,6) SWCNT and (f) sodium laurate-(7,6) SWCNT.

4.2. Effect of poly(diallyldimethylammonium chloride) (PDADMAC) on surfactant-SWCNT systems

PDADMAC is a strong cationic polyelectrolyte. The PDADMAC we used in this experiment has average Mw 200,000-350,000 (medium molecular weight) and the concentration is 20 wt. % in H_2O. In this experiment, we investigated the effect of PDADMAC on surfactant-SWCNT systems.

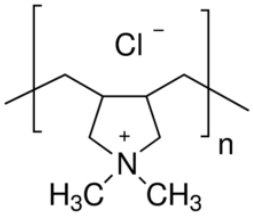

Figure 4.3 Structure of PDADMAC.

4.2.1. Effect of PDADMAC on SC-(7,6) SWCNT and SC-(6,5) SWCNT

PDADMAC solutions were added into surfactant-SWCNTs at various concentrations. After PDADMAC addition, the black flocculation appeared in the mixture (Appendix A). Since the carbon nanotubes dispersed using SC molecules display negative surface potential, SC-SWCNTs show attractive interactions to cationic polymer PDADMAC, which could crosslink nanotubes resulting in flocculation[4]. Both SC-(7,6) SWCNT and SC-(6,5) SWCNTs upon addition of PDADMAC showed black flocculation, and the photoluminescence was substantially quenched compared to the control solution without PDADMAC. Similar fluorescence quenching has been reported in aggregation induced suspensions[1] .

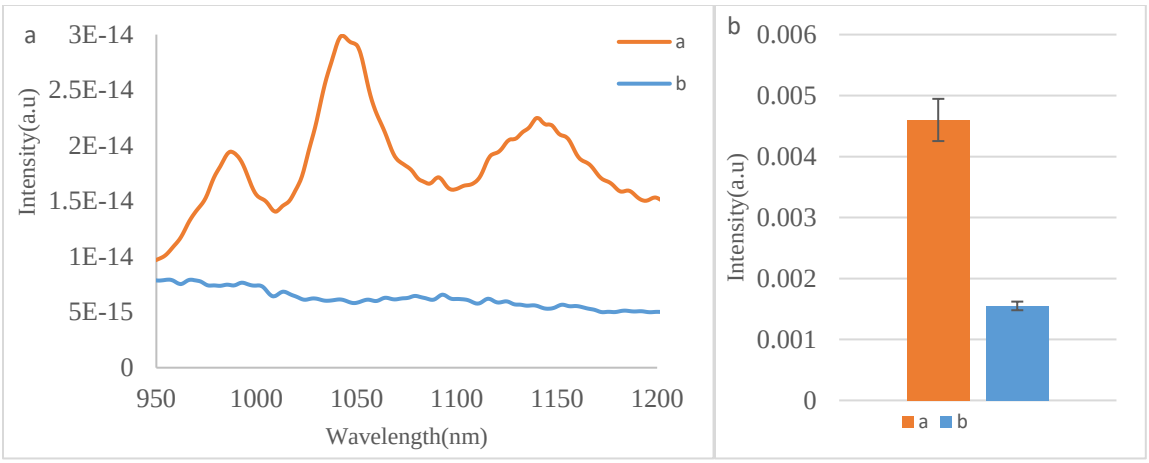

Figure 4.4 Effect of PDADMAC addition on SC-(7,6) SWCNT fluorescence (a) Orange line (Curve a) represents the fluorescence of SC-(7,6) SWCNT whereas blue line (Curve b) represents the spectra of SC-(7,6) SWCNT after addition of 100µL 2% PDADMAC solution. (b) Corresponding intensity of SC-(7,6) SWCNT with 100µL 2% PDADMAC solution and control SC-(7,6) SWCNT with addition of 100µL water.

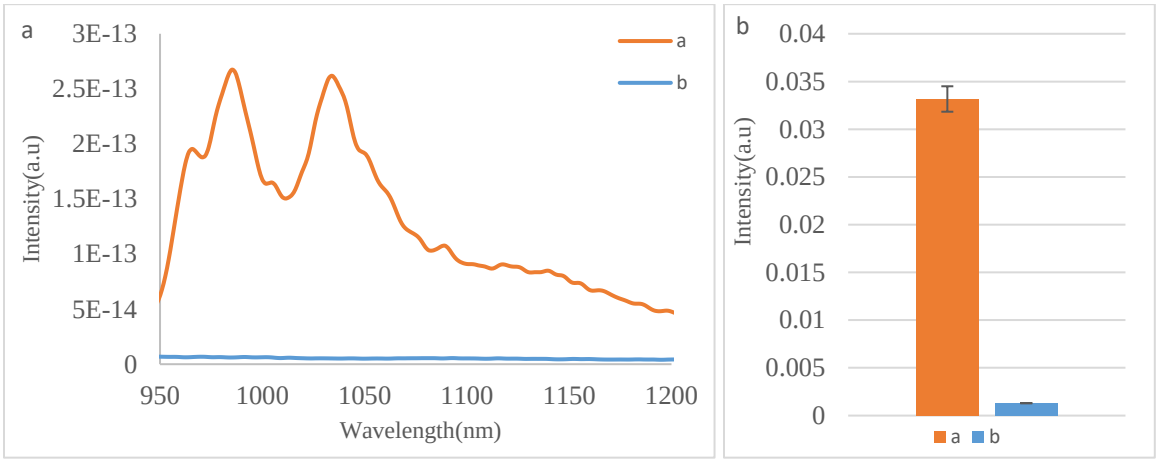

Figure 4.5 Effect of PDADMAC addition on SC-(6,5) SWCNT fluorescence (a) Orange line (Curve a) represents the fluorescence of SC-(6,5) SWCNT whereas blue line (Curve b) represents the spectra of SC-(6,5) SWCNT after addition of 100µL 2% PDADMAC solution. (b) Corresponding intensity of SC-(6,5) SWCNT with 100µL 2% PDADMAC solution and control SC-(6,5) SWCNT with addition of 100µL water.

4.2.2. Effect of PDADMAC on SDS-(7,6) SWCNT and SDS-(6,5) SWCNT

For SDS-SWCNT, similar phenomenon was observed. However, compared to SC-SWCNT, the degree of flocculation was less and some nanotubes remain freely dispersed in solution upon addition of the polycationic polymer, PDADMAC . Although there was aggregation in solution, the fluorescence increased. For SDS-(7,6), the spectra changed from flat and noisy to structured and sharp. For SDS-(6,5), the overall intensity of fluorescence has increased. This observation with sulfonated surfactant-SWCNTs is unprecedented. Future studies will investigate to enable a detailed mechanistic understanding on this topic.

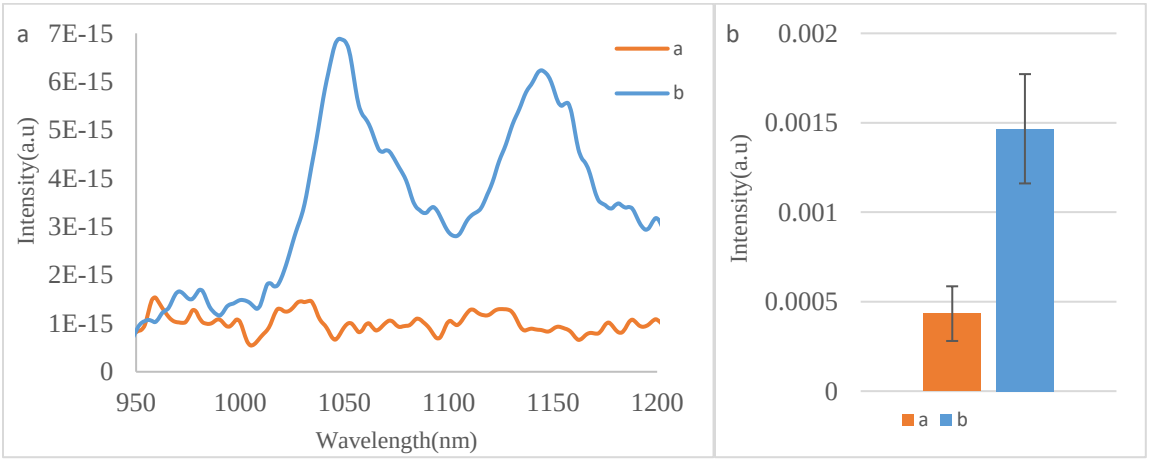

Figure 4.6 Effect of PDADMAC addition on SDS-(7,6) SWCNT fluorescence (a) Orange line (Curve a) represents the fluorescence of SDS-(7,6) SWCNT whereas blue line (Curve b) represents the spectra of SDS-(7,6) SWCNT after addition of 100µL 2% PDADMAC solution. (b) Corresponding intensity of SDS-(7,6) SWCNT with 100µL 2% PDADMAC solution and control SDS-(7,6) SWCNT with addition of 100µL water.

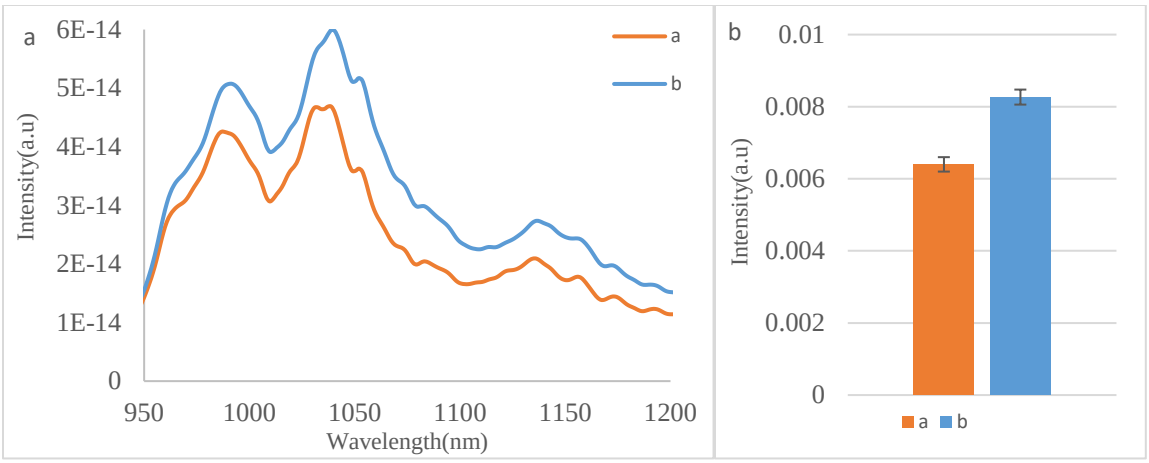

Figure 4.7 Effect of PDADMAC addition on SDS-(6,5) SWCNT fluorescence (a) Orange line (Curve a) represents the fluorescence of SDS-(6,5) SWCNT whereas blue line (Curve b) represents the spectra of SDS-(6,5) SWCNT after addition of 100µL 2% PDADMAC solution. (b) Corresponding intensity of SDS-(6,5) SWCNT with 100µL 2% PDADMAC solution and control SDS-(6,5) SWCNT with addition of 100µL water.

4.2.3. Effect of PDADMAC on SDBS-(7,6) SWCNT and sodium laurate- (7,6) SWCNT

Similar phenomenon, as discussed in section 4.2.1 was observed in SDBS-(7,6) SWCNT and sodium laurate-(7,6) SWCNT. Sodium laurate with carboxylic groups showed fluorescence quenching upon addition of PDADMAC (Figure 4.8), while SDBS with sulfonate groups yielded overall fluorescence enhancement upon addition of PDADMAC (Figure 4.9). Interestingly, the fluorescence enhancement of SDBS-SWCNT was found to be nanotube chirality dependent. The fluorescence of (7,6) SWCNT decreased while that of (7,5) SWCNT showed a strong enhancement. Due to shuttle differences on photophysical properties of nanotubes, chirality-dependent optical responses have been observed by many researchers in the field.

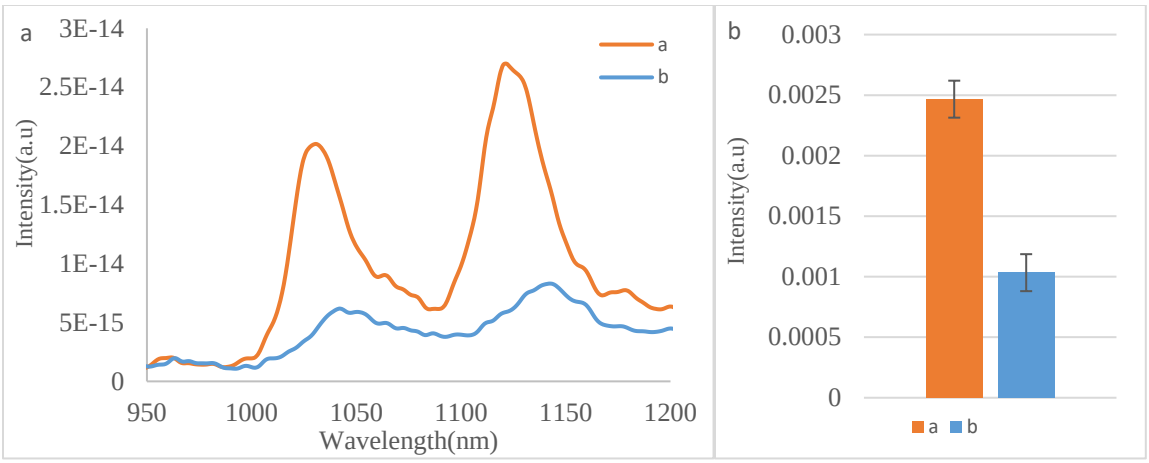

Figure 4.8 Effect of PDADMAC addition on sodium laurate-(7,6) SWCNT fluorescence (a) Orange line (Curve a) represents the fluorescence of sodium laurate-(7,6) SWCNT whereas blue line (Curve b) represents the spectra of sodium laurate-(7,6) SWCNT after addition of 100µL 2% PDADMAC solution. (b) Corresponding intensity of sodium laurate-(7,6) SWCNT with 100µL 2% PDADMAC solution and control of sodium laurate- (7,6) SWCNT with addition of 100µL water.

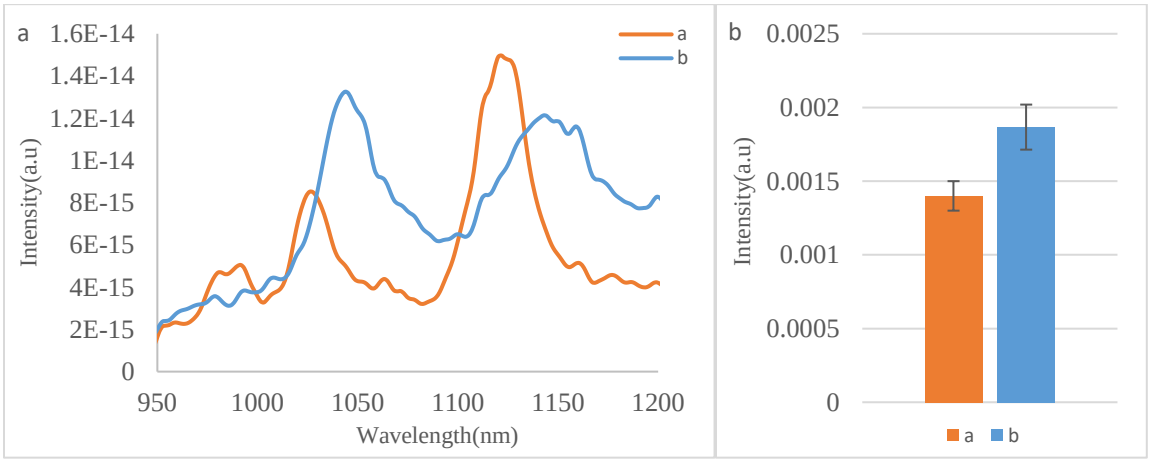

Figure 4.9 Effect of PDADMAC addition on SDBS-(7,6) SWCNT fluorescence (a) Orange line (Curve a) represents the fluorescence of SDBS-(7,6) SWCNT whereas blue line (Curve b) represents the spectra of SDBS-(7,6) SWCNT after addition of 100µL 2% PDADMAC solution. (b) Corresponding intensity of SDBS-(7,6) SWCNT with 100µL 2% PDADMAC solution and control of SDBS- (7,6) SWCNT with addition of 100µL water.

4.3. Effect of poly(allylamine hydrochloride) (PAH) on surfactant-SWCNT systems

The PAH we used in this experiment is a white powder and has an average Mw ~ 17500. It is a cationic polyelectrolyte and the electropositive character depends on the pH of the solution. Primary amine functional group is protonated at lower pH and unprotonated at higher pH. At neutral pH, primary amine groups remain protonated, making this polymer (PAH) moderately positively charged in water. It is soluble in water at room temperature. In this experiment, we investigated the effect of PAH addition on the fluorescence on two surfactant-SWCNT systems.

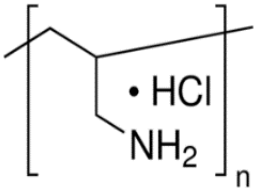

Figure 4.10 Structure of PAH

4.3.1. Effect of PAH on SC-(7,6) SWCNT and SC-(6,5) SWCNT

The effects of PAH on SC-SWCNT are similar to those observed in section 4.2.1. Once PAH was added to SC-SWCNTs, nanotubes were flocculated, and the fluorescence was quenched. For SC-(7,6) SWCNT, the quenching caused by PAH addition was not as strong as the addition of PDADMAC.

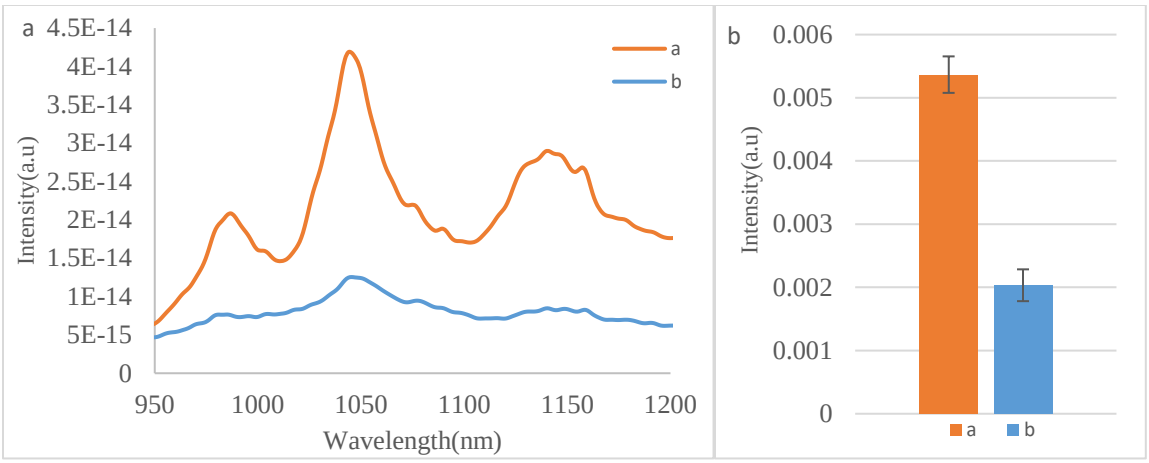

Figure 4.11 Effect of PAH addition on SC-(7,6) SWCNT fluorescence (a) Orange line (Curve a) represents the fluorescence of SC-(7,6) SWCNT whereas blue line (Curve b) represents the spectra of SC-(7,6) SWCNT after addition of 100µL 2% PAH solution. (b) Corresponding intensity of SC-(7,6) SWCNT with 100µL 2% PAH solution and control SC- (7,6) SWCNT with addition of 100µL water.

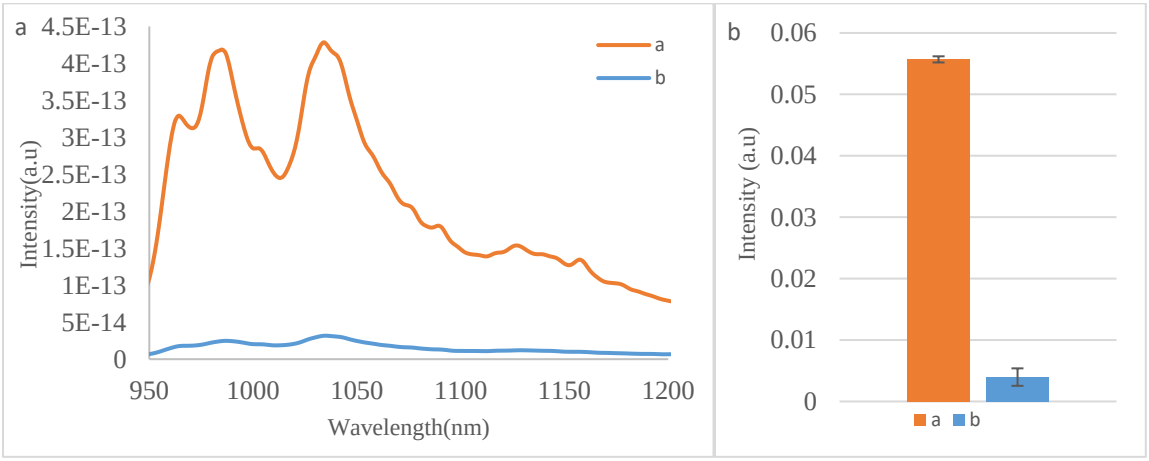

Figure 4.12 Effect of PAH addition on SC-(6,5) SWCNT fluorescence (a) Orange line (Curve a) represents the fluorescence of SC-(6,5) SWCNT whereas blue line (Curve b) represents the spectra of SC-(6,5) SWCNT after addition of 100µL 2% PAH solution. (b) Corresponding intensity of SC-(6,5) SWCNT with 100µL 2% PAH solution and control SC- (6,5) SWCNT with addition of 100µL water.

4.3.2. Effect of PAH on SDS-(7,6) SWCNT and SDS-(6,5) SWCNT

The black and white aggregation accompanied with fluorescence quenching was observed upon the addition of PAH into SDS-SWCNT (Figure 4.13 and figure 4.14). However, this quenching is not as strong as SC- SWCNT.

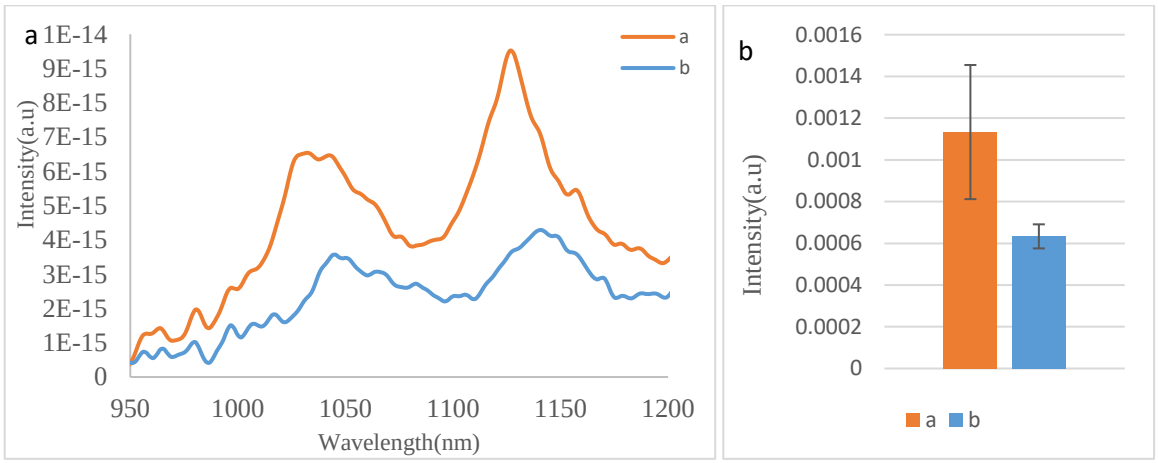

Figure 4.13 Effect of PAH addition on SDS-(7,6) SWCNT fluorescence (a) Orange line (Curve a) represents the fluorescence of SDS-(7,6) SWCNT whereas blue line (Curve b) represents the spectra of SDS-(7,6) SWCNT after addition of 100µL 2% PAH solution. (b) Corresponding intensity of SDS-(7,6) SWCNT with 100µL 2% PAH solution and control SDS- (7,6) SWCNT with addition of 100µL water

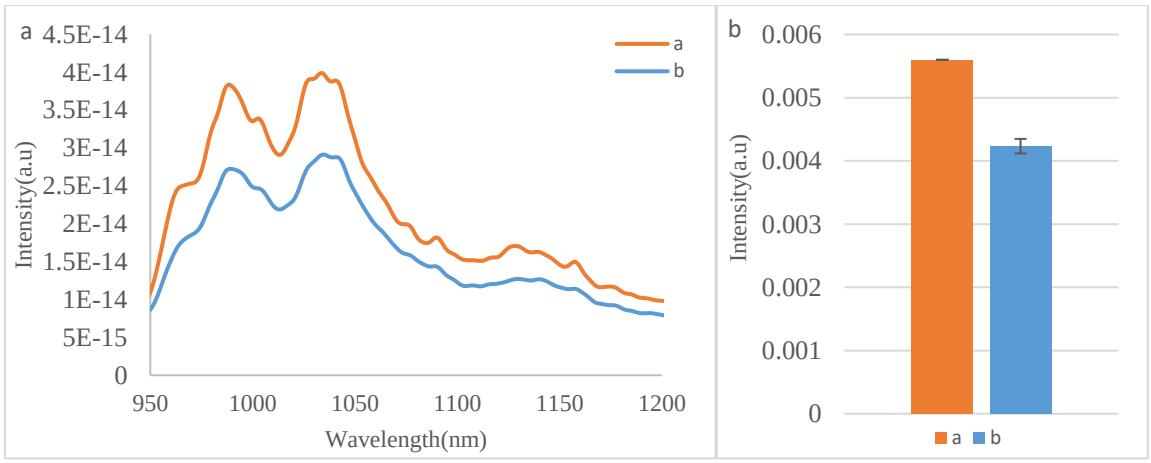

Figure 4.14 Effect of PAH addition on SDS-(6,5) SWCNT fluorescence (a) Orange line (Curve a) represents the fluorescence of SDS-(6,5) SWCNT whereas blue line (Curve b) represents the spectra of SDS-(6,5) SWCNT after addition of 100µL 2% PAH solution. (b) Corresponding intensity of SDS-(6,5) SWCNT with 100µL 2% PAH solution and control SDS- (6,5) SWCNT with addition of 100µL water.

4.3.3. Effect of PAH on SDBS-(7,6) SWCNT and sodium laurate-(7,6) SWCNT

2% PAH solution was added into SDBS-(7,6) SWCNT solution and sodium laurate-(7,6) SWCNT soluiton. Similar results were obtained when using the same method to process SDBS and sodium laurate. Both SDBS- (7,6) SWCNT and sodium laurate-(7,6) SWCNT were quenched with the addition of a PAH solution. sodium laurate which has carboxylic groups produced strong fluorescence quenching compare with SDBSs which has sulfonate groups.

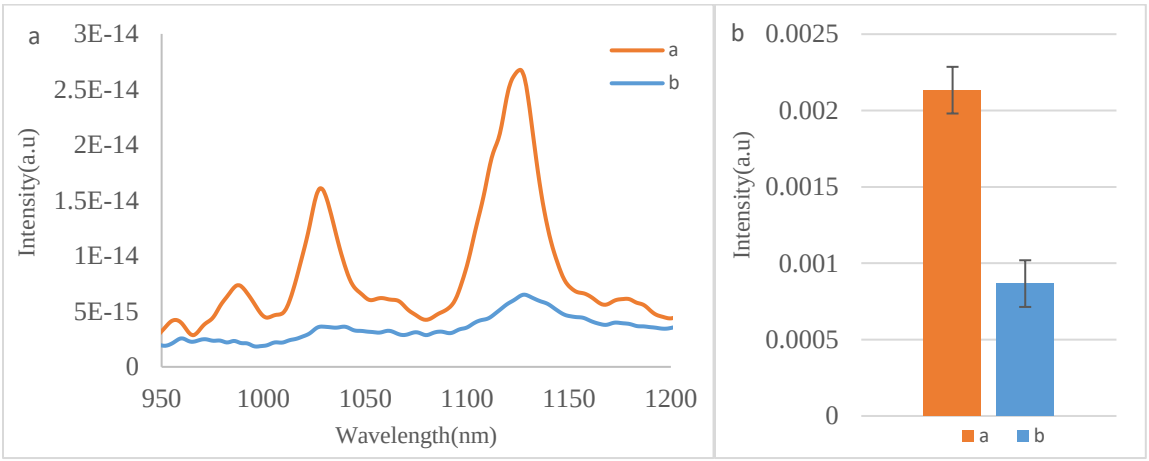

Figure 4.15 Effect of PAH addition on SDBS-(7,6) SWCNT fluorescence (a) Orange line (Curve a) represents the fluorescence of SDBS-(7,6) SWCNT whereas blue line (Curve b) represents the spectra of SDBS-(7,6) SWCNT after addition of 100µL 2% PAH solution. (b) Corresponding intensity of SDBS-(7,6) SWCNT with 100µL 2% PAH solution and control SDBS- (7,6) SWCNT with addition of 100µL water.

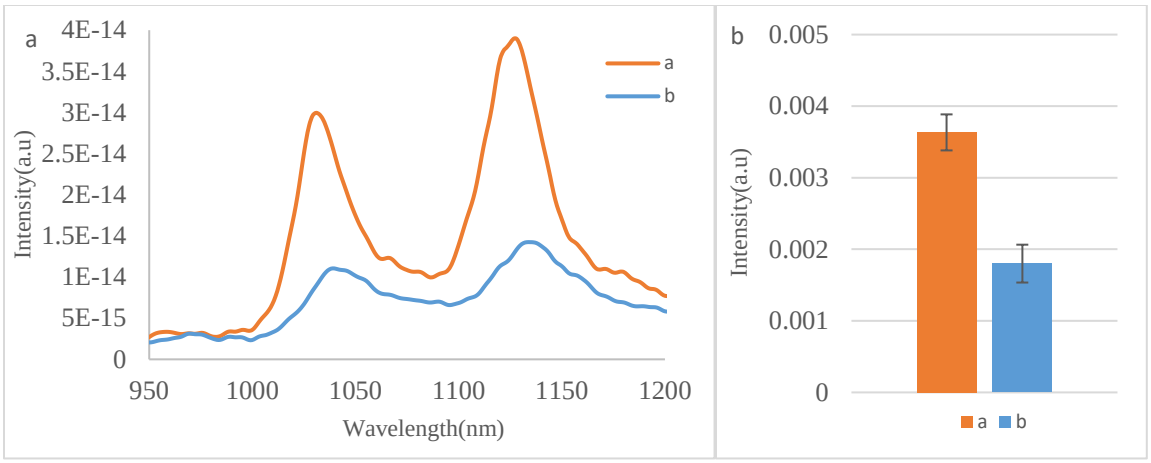

Figure 4.16 Effect of PAH addition on sodium laurate-(7,6) SWCNT fluorescence (a) Orange line (Curve a) represents the fluorescence of sodium laurate-(7,6) SWCNT whereas blue line (Curve b) represents the spectra of sodium laurate-(7,6) SWCNT after addition of 100µL 2% PAH solution. (b) Corresponding intensity of sodium laurate-(7,6) SWCNT with 100µL 2% PAH solution and control sodium laurate- (7,6) SWCNT with addition of 100µL water.

4.4. Effect of poly acrylic acid (PAA) on surfactant-SWCNT systems

In the previous sections, we observed that addition of positively charged polymers to anionic surfactant nanotubes caused a huge optical response. We hypothesized that this optical response is because of reorganization of surfactant molecules that exposes nanotube surfaces to the solvent (water) at various degrees. Solvent composition has been found to play a crucial role in nanotube's photoluminescence[2]. In order to test our hypothesis that if surfactant molecules do not undergo a significant reorganization on nanotube surfaces, optical changes will be modest, we designed the following experiment: poly(acrylic acid sodium salt) which is negatively charged polymer in water (at pH 7), was added to SDBS-(7,6) SWCNT and sodium laurate-(7,6) SWCNT solution and the change in fluorescence was evaluated.

Poly(acrylic acid sodium salt), shown in figure 4.17, is white (or light yellow) solid soluble in water at room temperature. The carboxylic group remains deprotonated at neutral and

basic pH conditions, forming a negatively charged polymer. At lower pH (acidic condition), carboxylic groups are protonated, forming a neutral polymer.

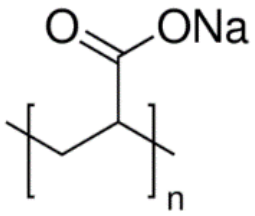

Figure 4.17 Structure of Poly(acrylic acid sodium salt)

4.4.1. Effect of PAA on SDBS-(7,6) SWCNT and sodium laurate-(7,6) SWCNT

The fluorescence intensity of SDBS-(7,6) remained virtually similar upon adding a PAA solution. There is a slight decrease in the intensity for sodium laurate-(7,6) SWCNT after adding the PAA solution. But compared to cationic polymers (Figure 4.15, 4.16), this change in intensity is not obvious. After adding a polymer with the similar charges as the surfactants, the fluorescence of the carbon nanotube solution did not change significantly.

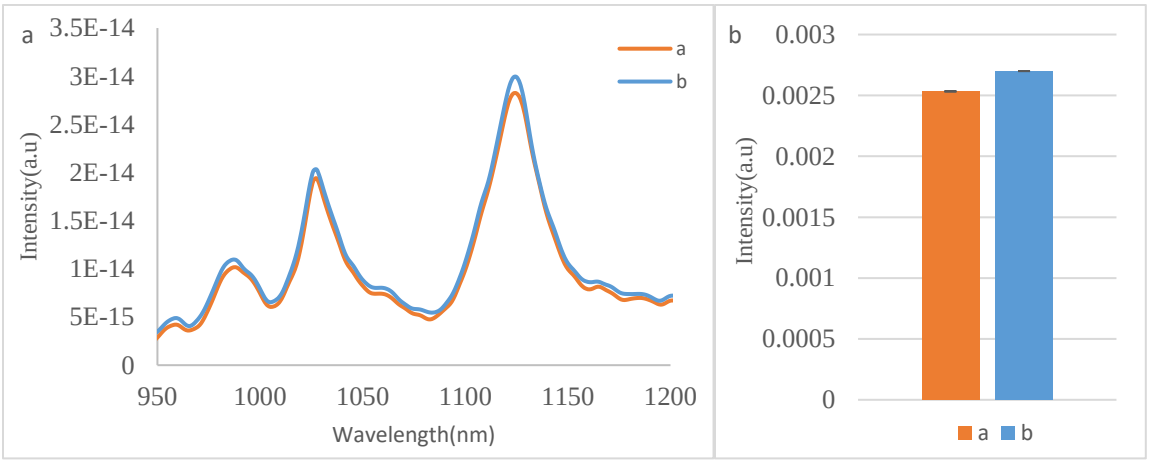

Figure 4.18 Effect of PAA addition on SDBS-(7,6) SWCNT fluorescence (a) Orange line (Curve a) represents the fluorescence of SDBS-(7,6) SWCNT whereas blue line (Curve b) represents the spectra of SDBS-(7,6) SWCNT after addition of 100µL 2% PAH solution. (b) Corresponding intensity of SDBS-(7,6) SWCNT with 100µL 2% PAH solution and control SDBS- (7,6) SWCNT with addition of 100µL water.

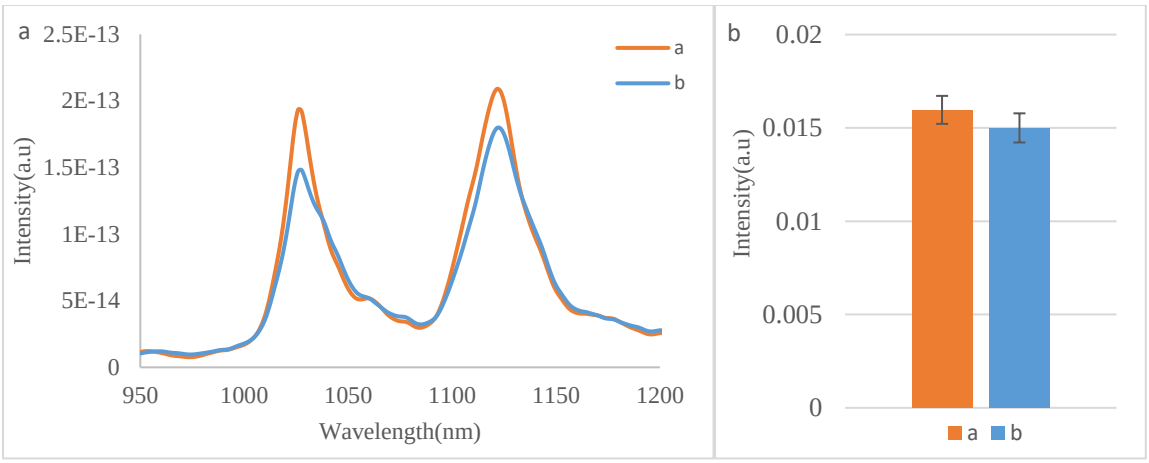

Figure 4.19 Effect of PAA addition on sodium laurate-(7,6) SWCNT fluorescence (a) Orange line (Curve a) represents the fluorescence of sodium laurate-(7,6) SWCNT whereas blue line (Curve b) represents the spectra of sodium laurate-(7,6) SWCNT after addition of 100µL 2% PAA solution. (b) Corresponding intensity of sodium laurate-(7,6) SWCNT with 100µL 2% PAA solution and control sodium laurate- (7,6) SWCNT with addition of 100µL water.

4.5. Discussion and conclusion

Previous research found that there are two main factors that will influence the fluorescence of surfactant-SWCNT: 1) the debundling ability of a surfactant and 2) the environment around SWCNT[58] . It has been reported that fluorescence of SWCNT is very sensitive to the environment of SWCNT[59]. Our experimental results are consistent with previous observations on different surfactants exhibiting variable influence on the SWCNT photoluminescence. Among the surfactant we used, SC which has large volume and carboxylate provides the strongest fluorescence intensity, and followed by sodium laurate, SDBS and SDS.

For the experiment of interaction of surfactant carbon nanotubes with different polymers, because the carbon nanotubes dispersed using SC, SDS, SDBS and sodium laurate molecules display negative surface potential, surfactant -SWCNTs show attractive interactions to cationic polymers, which could crosslink nanotubes resulting in flocculation[60]. Previous studies have found that the aggregation of carbon nanotubes is often accompanied by fluorescence quenching.

However, we found for the first time that the fluorescence intensity of carbon nanotubes dispersed with sulfonated (sulfonic acid groups) surfactants increased after strong cationic polymers (such as PDADMAC) were added, and it also accompanied by aggregation. We also found that when a polymer with the like charge as the surfactant (e.g., PAA) was added, the fluorescence intensity of the carbon nanotube solution does not change significantly. Here, we make a hypothesis (Figure 4.20): the addition of cationic polymers will interact with negatively charged surfactants, causing those surfactant molecules dislodge from the surface of carbon nanotubes. When polymer concentration is increased, a large amount of surfactant molecules detach from the surface of the carbon nanotubes, so the carbon nanotubes will re-aggregate together and form black aggregates due to the hydrophobicity. When the carbon nanotubes aggregate, the fluorescence is quenched. At the same time, the detachment of the surfactant causes the water molecules to re-aggregate on the surface of the carbon nanotubes, which also produces fluorescence quenching[61]. However, the fluorescence enhancement was observed in the SDS and SDBS carbon nanotube systems, which may indicate that the accumulation of sulfonate groups on the surface of the carbon nanotubes will cause fluorescence quenching. The addition of a strongly positive charged polymer (PDADMAC) greatly attenuated this quenching and compensated for the quenching caused by the reason above, so an increase in fluorescence was observed. However, the ability of weakly positive charged polymer (PAH) to adsorb sulfonate-surfactant is not enough to compensate the quenching, so a certain degree of fluorescence quenching is observed. This may provide a new idea for the design of carbon nanotube biosensors.

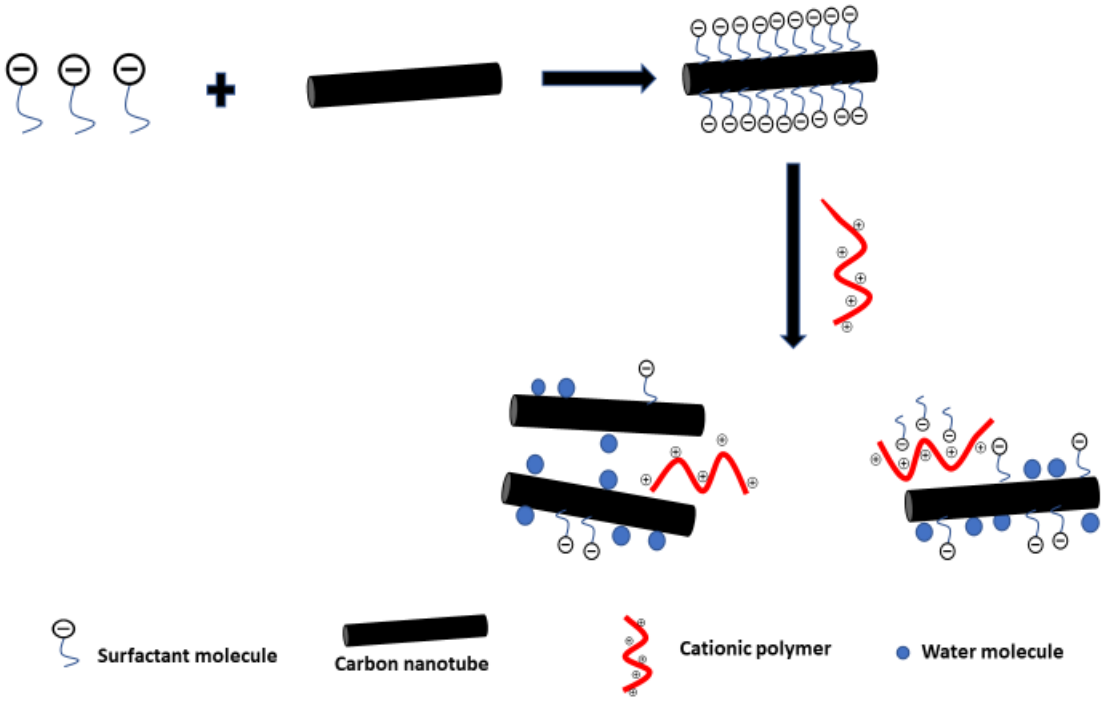

Figure 4.20 Scheme for the mechanism of the fluorescence enhancement and quenching of surfactant- SWCNT upon the addition of cationic polymers.

4.6. PSS- (6,5) SWCNT as an optical sensor

Based on the experiment above, we design a molecular sensor based on carbon nanotubes for protamine. Protamine, as an antibody to heparin, has strong reactivity to sulfonate groups. Poly(sodium 4-styrenesulfonate) (PSS) polymer (Figure 4.21) with benzene ring and sulfonate group has been previously reported to disperse SWCNT. However, the study did not report optical characteristics of the sample. We found that PSS suspends both (6,5) and (7,6) enriched SWCNTs. Furthermore, we found that (6,5) SWCNT provides stronger fluorescence intensity compared to (7,6) SWCNT prepared under the same experimental conditions. Thus we choose PSS (6,5) SWCNT to test the feasibility to apply it as a molecular sensor for protamine.

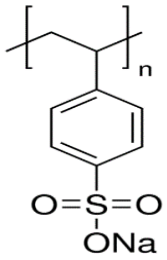

Figure 4.21 Structure of Poly(sodium 4-styrenesulfonate)

The concentration of carbon nanotubes in solution was determined via UV-Vis-NIR absorbance spectroscopy using the extinction coefficient Abs_{630} = 0.036 $Lmg^{-1}cm^{-1}$ (Appendix B). The concentration of PSS-(6,5) SWCNT sample was 183.3316mg/L. The stock solution was diluted 10-folds in water and used for experiments.

4.6.1. Effect of PDADMAC and PAH on PSS-(6,5) SWCNT

The NIR fluorescence measurements on PSS-(6,5) SWCNT showed no discernable peaks as compared to surfactant- (6,5) SWCNT solutions. Two synthetic cationic polymers, PDADMAC and PAH, and a biopolymer protamine were then added to the PSS-SWCNT separately. After addition of PDADMAC solution there was a significant increase in the fluorescence intensity (Figure 4.22). This showed that PSS-(6,5) SWCNT has similar properties as SDS-SWCNT and SDBS-SWCNT, and the increase in fluorescence intensity is stronger. The addition of PAH solution also made the intensity increased, which is different with surfactant-SWCNT (Figure 4.22).

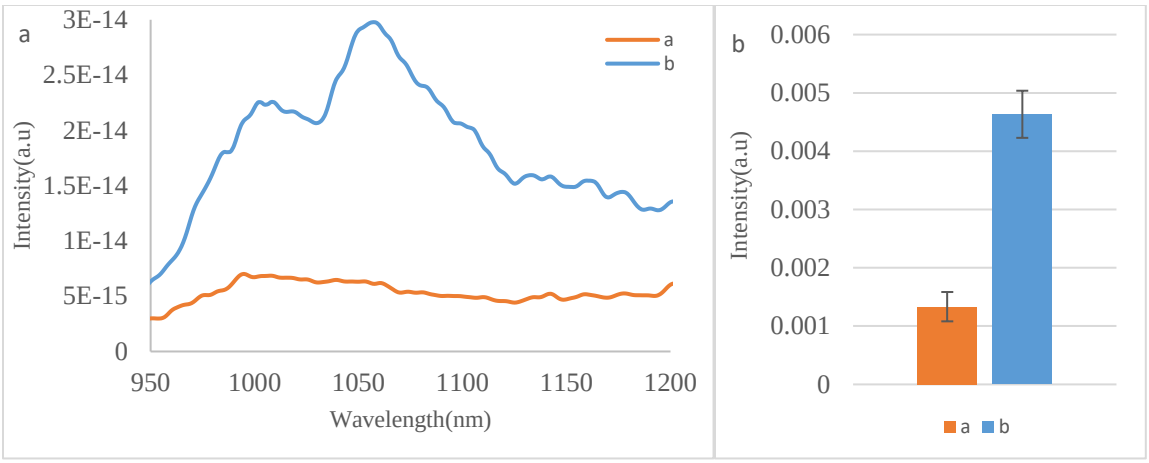

Figure 4.22 Effect of PDADAC on PSS-(6,5) SWCNT fluorescence. (a) Orange line (Curve a) represents the fluorescence of PSS-(6,5) SWCNT whereas blue line (Curve b) represents the spectra of PSS-(6,5) SWCNT after addition of 100µL 2% PDADMAC solution. (b) Corresponding intensity of PSS-(6,5) SWCNT with 100µL 2% PDADMAC solution and control PSS- (6,5) SWCNT with addition of 100µL water.

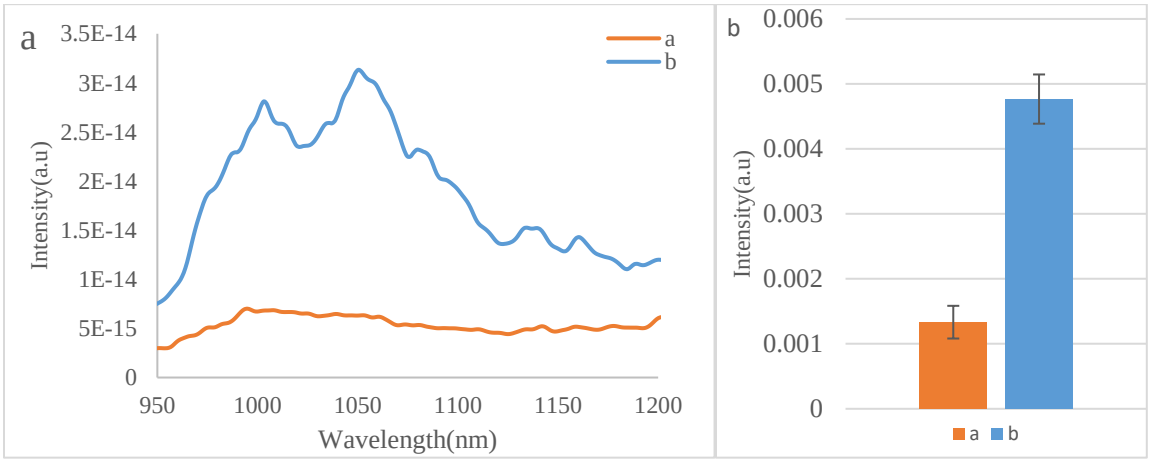

Figure 4.23 Effect of PAH on PSS-(6,5) SWCNT fluorescence. (a) Orange line (Curve a) represents the fluorescence of PSS-(6,5) SWCNT whereas blue line (Curve b) represents the spectra of PSS-(6,5) SWCNT after addition of 100µL 2% PAH solution. (b) Corresponding intensity of PSS-(6,5) SWCNT with 100µL 2% PAH solution and control PSS- (6,5) SWCNT with addition of 100µL water.

4.6.2. Effect of protamine on PSS- (6,5) SWCNT

The fluorescence intensity changes of different concentration of protamine to PSS- (6,5) SWCNT was measured in this section. Since this is the first time PSS- (6,5) SWCNT is used as a

protamine biosensor, the applicable concentration is unknown. Initially experiment with protamine was in a larger concentration range, then continued to narrow the concentration range of protamine.

4.6.2.1 Effect of protamine (0-2500mg/L) on PSS-(6,5) SWCNT

To investigate the reaction of PSS-(6,5) SWCNT with protamine, five different concentration of protamine were chosen: 50mg/L, 100mg/L, 125mg/L, 2000mg/L and 2500mg/L (refer to the concentration of protamine in nanotubes solution) and the fluorescence was shown in figure 4.24 With the increasing of protamine concentration, the fluorescence intensity of nanotube solution also increased. However, this change was not linear. The fluorescence intensity from 0mg/L-125mg/L showed a certain linear change. When the concentration reached to 2000mg/L, the change of fluorescence intensity no longer following the linear change.

After protamine addition, black and white flocculation appeared in the solution, and is much more than the SWCNT solution with PDADMAC or PAH. The carbon nanotube solution became cloudy after adding protamine.

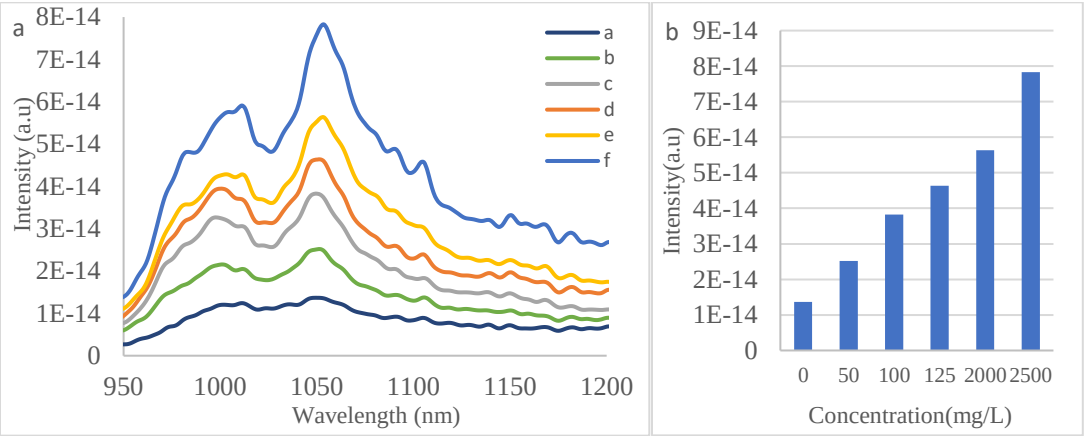

Figure 4.24 Effect of protamine on PSS-(6,5) SWCNT fluorescence. (a) a: PSS-(6,5) SWCNT with 100µL PBS solution. b: PSS-(6,5) SWCNT with 100µL 50mg/L protamine. c: PSS-(6,5) SWCNT with 100µL 100mg/L protamine. d: PSS-(6,5) SWCNT with 125mg/L protamine. e: PSS-(6,5) SWCNT with 2000mg/L. f: PSS-(6,5) SWCNT with 2500mg/L. (b) Corresponding intensity of PSS-(6,5) SWCNT with different concentration of protamine (mg/L).

4.6.2.2 Effect of protamine (0-1000mg/L) on PSS-(6,5) SWCNT

Based on the previous experiment, this experiment narrowed the range of protamine concentration, and each experiment was triplicated. Samples with five different concentration were tested: 50mg/L, 100mg/L, 200mg/L, 500mg/L and 1000mg/L (refer to the concentration of protamine in nanotubes solution). The linear change was observed between the concentration of 0mg/L-500mg/L. However, the fluorescence intensity decreased when the concentration of protamine increased from 500mg/L to 1000mg/L. It is also found that the fluorescence intensity of the 1000mg/L concentration solution was inconsistent over time (ca. 1 h) and varied among batches of solutions prepared (See below).

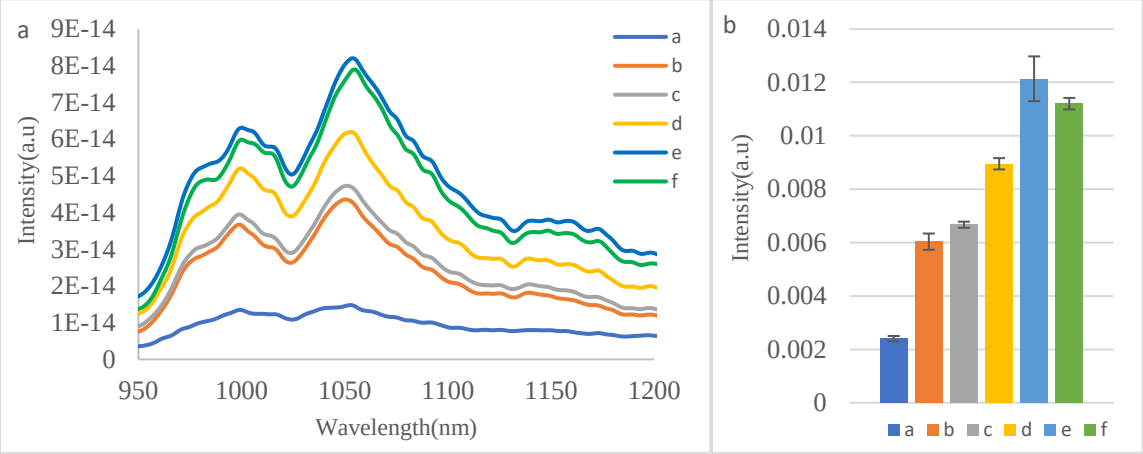

Figure 4.25 Effect of protamine on PSS-(6,5) SWCNT fluorescence. (a) Emission spectra and (b) Corresponding intensity of PSS-(6,5) SWCNT with different concentration of protamine (mg/L). a: PSS-(6,5) SWCNT with 100µL PBS solution. b: PSS-(6,5) SWCNT with 100µL 50mg/L protamine. c: PSS-(6,5) SWCNT with 100µL 100mg/L protamine. d: PSS-(6,5) SWCNT with 200mg/L protamine. e: PSS-(6,5) SWCNT with 500mg/L. f: PSS-(6,5) SWCNT with 1000mg/L. All experiments were performed in triplicate and each spectrum represents an average of three measurements.

4.6.2.3 Effect of protamine (1000mg/L) on PSS-(6,5) SWCNT

To further investigate the fluorescence intensity fluctuation that was observed in section 4.6.3, eight different samples of the PSS-(6,5) SWCNT of exact same concentration were

prepared following the same method of preparation for each sample. The fluorescence of those eight PSS- (6,5) SWCNT solution was measured. The 1000mg/L protamine with PSS-(6,5) SWCNT solution has a wide range of fluorescence intensity (Figure 4.26). These samples were unstable, shaking or stationary solution will make the fluorescence changed.

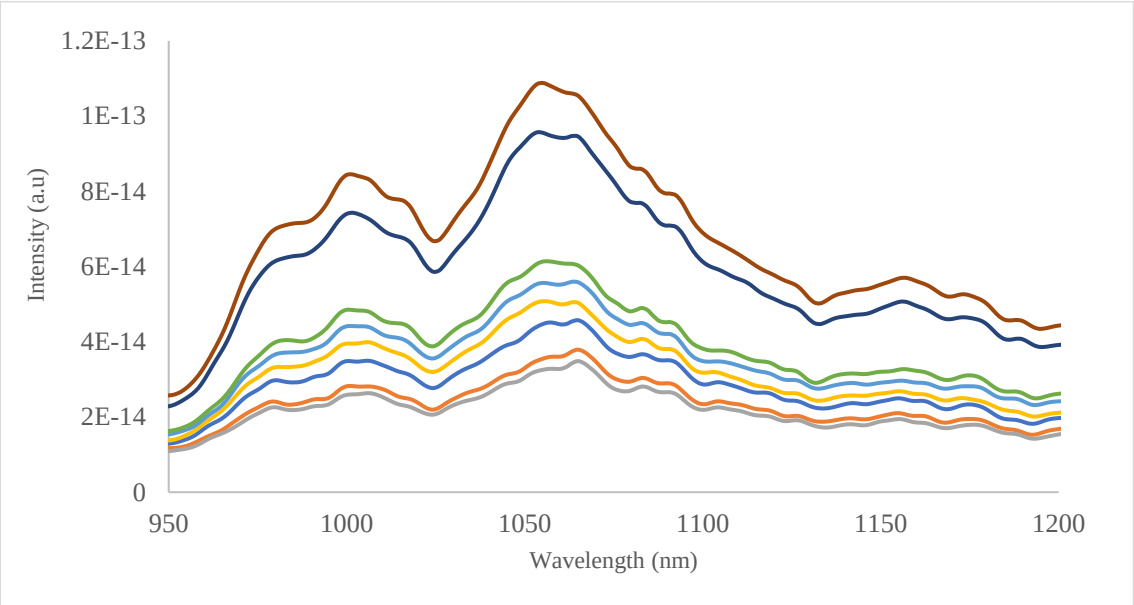

Figure 4.26 Representative spectra of PSS-(6,5) SWCNT with 1000mg/L protamine.

4.6.2.4 Effect of protamine (0-30mg/L) on PSS-(6,5) SWCNT

The analysis of the low concentration range protamine solution found that the change in fluorescence intensity was distinct with as low as 5 mg/L protamine. The fluorescence intensity increased between 5-30mg/L except with one sample (15mg/L) being an outlier. The change of fluorescence intensity with protamine concentration was not linear. Similar trend was observed when the concentration of nanotubes was doubled. For this case, fluorescence intensity decreased between 20-25mg/L and increased again after the concentration reach to 30mg/L. This showed that this change was relative to the concentration of nanotubes.

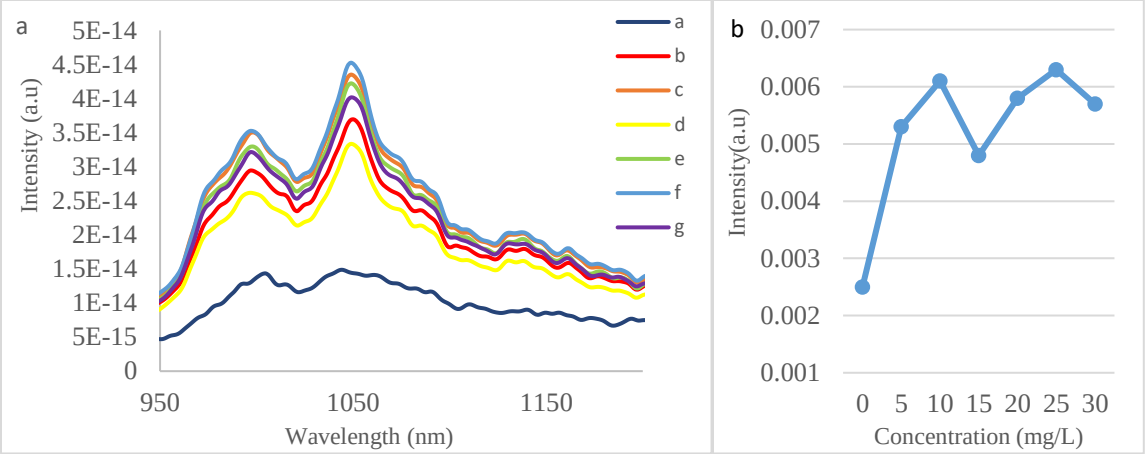

Figure 4.27 Effect of protamine on PSS-(6,5) SWCNT fluorescence. (a) a: PSS-(6,5) SWCNT with 100μL PBS solution. b: PSS-(6,5) SWCNT with 100μL 5mg/L protamine. c: PSS-(6,5) SWCNT with 100μL 10mg/L protamine. d: PSS-(6,5) SWCNT with 15mg/L protamine. e: PSS-(6,5) SWCNT with 20mg/L. f: PSS-(6,5) SWCNT with 25mg/L. g: PSS-(6,5) SWCNT with 30mg/L. (b) Intensity change of PSS-(6,5) SWCNT with different concentration of protamine.

4.6.3. Kinetics experiment of PSS-(6,5) SWCNT with 50mg/L protamine

Based on the experiment above, 50mg/L protamine was chosen to conduct the kinetics measurements experiment. The purpose of this experiment is to obtain the time required for the interaction between protamine and carbon nanotube solution to reach equilibrium. It is found that the fluorescence intensity exhibited plateau after 25mins. The control sample (without protamine) remained stable throughout the experiment. There were a few minutes (< 5 minutes) time lag between the sample preparation and data collection, which might have caused the initial differences in the intensity between the control and treated samples (Figure 4.27).

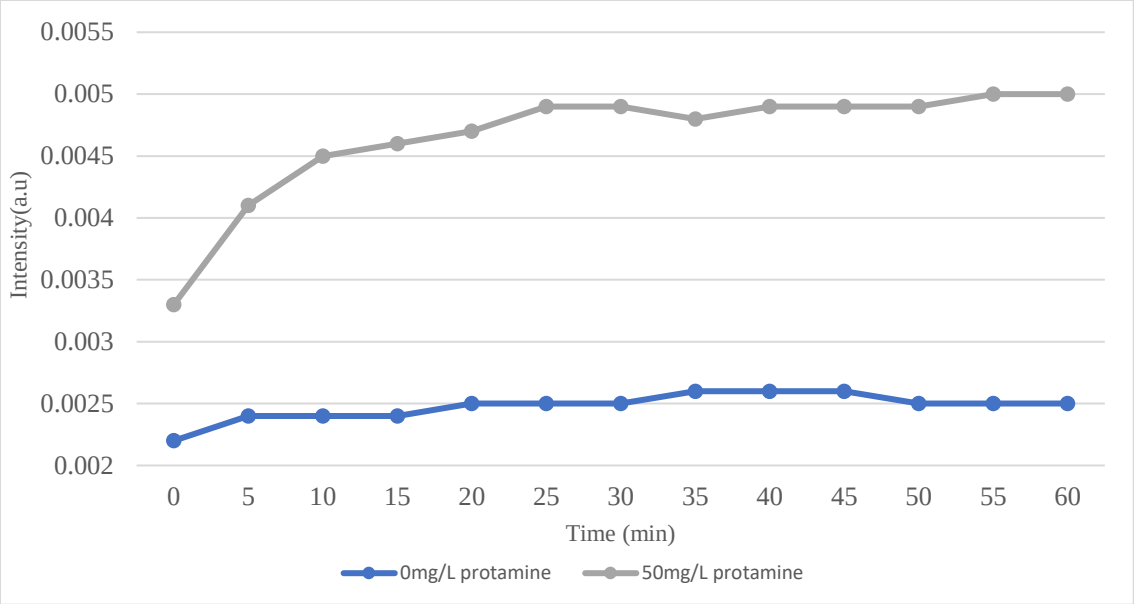

Figure 4.28 Fluorescence intensity change of PSS-(6,5) SWCNT relative to the time change after addition of 50mg/L protamine.

4.6.4 PSS-(6,5) SWCNT with 0.02% PDADMAC, PAH and Protamine

To evaluate the response of PSS- (6,5) SWCNT, PDADMAC, PAH and protamine (at the same (weight/vol) concentration) solution were added into PSS- (6,5) SWCNT. The result showed that protamine changes the fluorescence intensity of PSS-(6,5) SWCNT most significantly compared to PDADMAC and PAH. 0.02% protamine can strongly increase the intensity while same concentration of PDADMAC and PAH remains virtually no change. A number of factors such as chemical composition, polymer molecular weight and molecular weight distribution may have influenced the interaction between the nanotube and added polymer. Further investigations are warranted for thorough understanding.

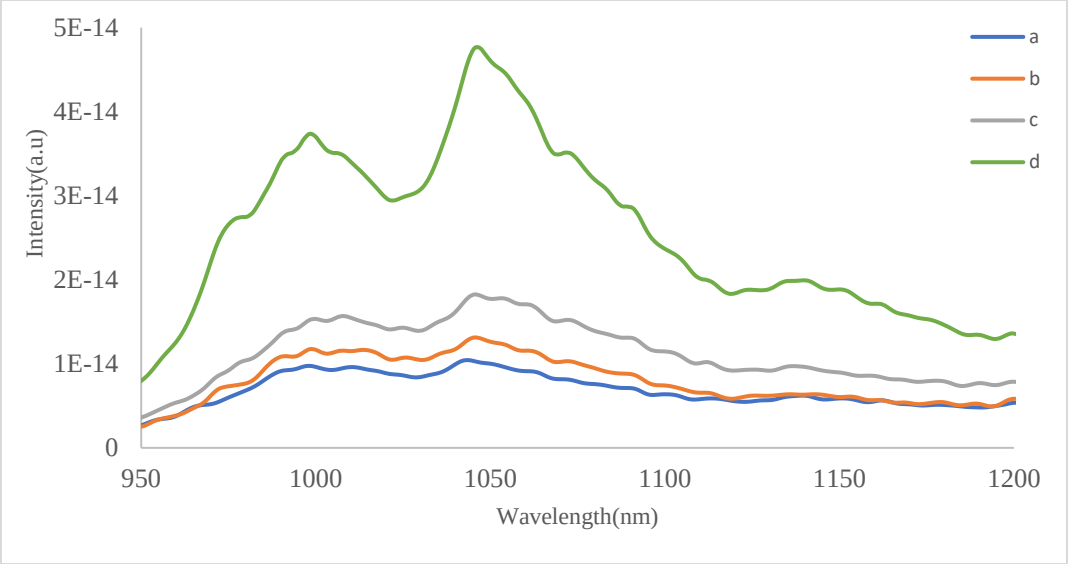

Figure 4.29 Representative spectra of PSS-(6,5) SWCNT after addition of 100µL 0.02% PDADMAC, 0.02% PAH and 0.02% protamine solution. a: PSS-(6,5) SWCNT with100µL PBS solution. b: PSS-(6,5) SWCNT with 100µL 0.02% PDADMAC solution. c: PSS-(6,5) SWCNT with 100µL 0.02% PAH solution. d: PSS-(6,5) SWCNT with 0.02% 100µL Protamine solution.

4.6.5. PAA-(6,5) SWCNT with 0.02% PDADMAC, PAH and protamine

We did a similar experiment as section in 4.6.4, but now using PAA- (6,5) SWCNT. The results showed that 0.02% PDADMAC and PAH had no significant effects on PAA- (6,5) SWCNT fluorescence intensity while 0.02% protamine drastically quenched the fluorescence. This result is consistent to the results we observed in the surfactant- SWCNT system (Section 4.6.4) with a distinct response was exhibited by protamine and not by other two polymers used in the experiment. Interestingly, we also found that the SWCNT dispersed by using carboxylic acid functionalized polymers when flocculated upon addition of a cationic polymer, the fluorescence intensity always found decrease. This is a stark contrast with PSS polymer-SWCNTs optical response. Further investigations are warranted for thorough understanding.

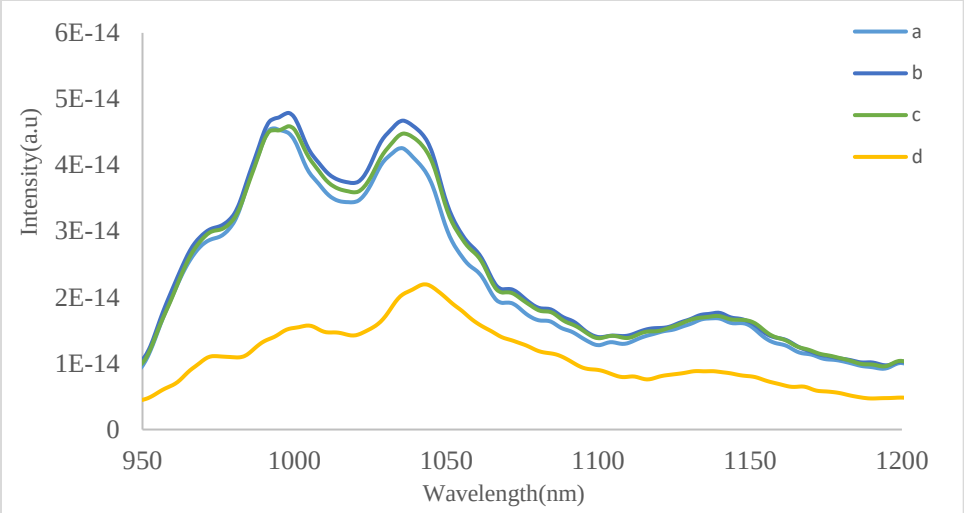

Figure 4.30 Representative spectra of PAA-(6,5) SWCNT after addition of 100µL 0.02% PDADMAC, 0.02% PAH and 0.02% protamine solution. a: PAA-(6,5) SWCNT with100µL PBS solution (Control). b: PAA-(6,5) SWCNT with 100µL 0.02% PDADMAC solution. c: PAA-(6,5) SWCNT with 100µL 0.02% PAH solution. d: PAA-(6,5) SWCNT with 0.02% 100µL Protamine solution.

4.6.6. Discussion and conclusion

We explored the feasibility of using carbon nanotubes to design protamine sensors. The results showed that PSS-(6,5) SWCNT has a strong response to cationic macromolecule which causes an enhancement of fluorescence intensity, while no obvious changes to negatively charged polymers. However, PAA- (6,5) SWCNT showed fluorescence quenching upon protamine addition. The mechanism for this enhancement or quenching may be different as compared to surfactant-SWCNT systems (Figure 4.32). Polymers such as PSS are not simply adsorbed on the surface of carbon nanotubes like surfactants but are bound to carbon nanotubes by wrapping[35]. After sonication and centrifugation, this binding is very stable, thus the polymer is difficult to separate from the carbon nanotubes. Therefore, even after the cationic macromolecule was added to enable charge interactions, the original dispersant polymer will remain adsorbed on the surface of the carbon nanotube. The adsorption of polymers on the

surface of carbon nanotubes will replace the water molecules on the surface, which increases the fluorescence intensity. This process also causes the sulfonate groups on the surface of carbon nanotubes to be shielded, so the fluorescence intensity is enhanced. The fluorescence of this complex was inconsistent when the protamine concentration was high (>1000mg/L), but it showed some linear change at low concentration. The concentration of carbon nanotubes will also affect this linear change. Compared with other cationic macromolecules such as PDADMAC and PAH, protamine has much stronger interaction with PSS-(6,5) SWCNT, which illustrate that this probe has strong selectivity toward protamine. However, due to the limitations of the experiment (lab shutdown amid COVID-19 situation), some experiments were conducted in limited attempts (sections; 3.6.3.1, 3.6.3.4, 3.6.5 and 3.6.6) and future investigations are warranted for sensitivity and selectivity. In general, we believe that carbon nanotubes have the potential to be protamine biosensors because it has strong sensitivity and specificity. However, the interaction mechanism and the applicable concentrations require further study.

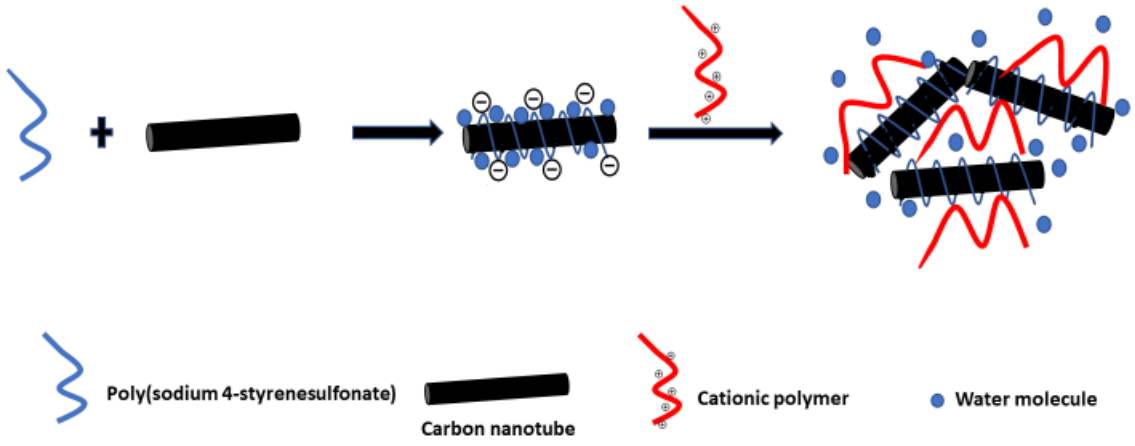

Figure 4.31 Scheme for the mechanism of fluorescence enhancement of PSS-SWCNT upon the addition of a cationic polymer.

CHAPTER 5

CONCLUSION AND OUTLOOK

The purpose for our research was to understand and explore the properties and applications of SWCNT for development of optical biosensors. Through spectral analysis of the complex of surfactant- SWCNT and cationic polymers, a fluorescence enhancement accompanied with aggregation of carbon nanotubes was observed for the first time, and it is in stark contrast to previous reports on carbon nanotube aggregation accompanied by fluorescence quenching. By using an anionic polymer as a comparison, we believe that this fluorescence enhancement or quenching is due to the difference in the charged groups of the polymer. We further found that the addition of cationic polymer to a solution of SWCNT dispersed with sulfonate group surfactant will produce fluorescence enhancement. Based on this property, we used PSS to disperse (6,5) SWCNT and designed a biosensor for protamine detection. Our initial investigations showed that the sensor exhibits extremely high sensitivity and moderate selectivity to protamine. We also proposed hypotheses about this unique phenomenon of fluorescence enhancement. We believed that the mechanism of this fluorescence enhancement is different in surfactant- SWCNT and in polymer wrapped- SWCNT.

This unique fluorescence enhancement provides a new idea for the design of SWCNT biosensors. Although we have proposed a possible mechanism hypothesis, the reason why the sulfonate group produces fluorescence quenching requires further investigations. Meanwhile, based on the several experimental results, a new optical sensor based on SWCNT has been designed for protamine detection. To the best of our knowledge this is the first NIR optical sensor for this important biomolecule. The sensor sensitivity and selectivity was found in good

range. All in all, the sensor still has a lot of room for optimization. The future research may focus on the shift in wavelength as well.

REFERENCES

1. Shao, L.; Gao, Y.; Yan, F. Semiconductor Quantum Dots for Biomedicial Applications. *Sensors (Basel, Switzerland)* **2011**, *11*, 11736-11751.

2. Ramgir, N. S.; Yang, Y.; Zacharias, M. Nanowire-Based Sensors. *Small* **2010**, *6*, 1705-1722.

3. Liu, Z.; Tabakman, S.; Welsher, K.; Dai, H. Carbon nanotubes in biology and medicine: In vitro and in vivo detection, imaging and drug delivery. *Nano Res* **2009**, *2*, 85-120.

4. Chen, Z.; Zhang, X.; Yang, R.; Zhu, Z.; Chen, Y.; Tan, W. Single-walled carbon nanotubes as optical materials for biosensing. *Nanoscale* **2011**, *3*, 1949-1956.

5. Boghossian , A. A.; Zhang , J.; Barone, P. W.; Reuel, N. F.; Kim, J.; Heller, D. A.; Ahn, J.; Hilmer, A. J.; Rwei, A.; Arkalgud, J. R.; Zhang, C. T.; Strano, M. S. Near-Infrared Fluorescent Sensors based on Single-Walled Carbon Nanotubes for Life Sciences Applications. *ChemSusChem* **2011**, *4*, 848-863.

6. Iijima, S. Helical microtubules of graphitic carbon. *Nature* **1991**, *354*, 56-58.

7. Ge, M.; Sattler, K. Vapor-Condensation Generation and STM Analysis of Fullerene Tubes. *Science* **1993**, *260*, 515-518.

8. Jena, P. V.; Galassi, T. V.; Roxbury, D.; Heller, D. A. Progress Towards Applications of Carbon Nanotube Photoluminescence. *ECS journal of solid state science and technology* **2017**, *6*, M3075-M3077.

9. Williams, R. M.; Lee, C.; Galassi, T. V.; Harvey, J. D.; Leicher, R.; Sirenko, M.; Dorso, M. A.; Shah, J.; Olvera, N.; Dao, F.; Levine, D. A.; Heller, D. A. Noninvasive ovarian cancer biomarker detection via an optical nanosensor implant. *Science advances* **2018**, *4*, eaaq1090.

10. Kruss, S.; Hilmer, A. J.; Zhang, J.; Reuel, N. F.; Mu, B.; Strano, M. S. Carbon nanotubes as optical biomedical sensors. *Advanced Drug Delivery Reviews* **2013**, *65*, 1933-1950.

11. Budhathoki-Uprety, J.; Shah, J.; Korsen, J. A.; Wayne, A. E.; Galassi, T. V.; Cohen, J. R.; Harvey, J. D.; Jena, P. V.; Ramanathan, L. V.; Jaimes, E. A.; Heller, D. A. Synthetic molecular recognition nanosensor paint for microalbuminuria. *Nature communications* **2019**, *10*, 3605-9.

12. Budhathoki-Uprety, J.; Langenbacher, R. E.; Jena, P. V.; Roxbury, D.; Heller, D. A. A Carbon Nanotube Optical Sensor Reports Nuclear Entry via a Noncanonical Pathway. *ACS Nano* **2017**, *11*, 3875-3882.

13. Tomas Frejka; Tomáš Sobotka Overview Chapter 1. *Demographic Research* **2008**, *19*, 15-46.

14. Proctor, J. E.; Melendrez Armada, D. A.; Vijayaraghavan, A. *Anœ introduction to graphene and carbon nanotubes;* CRC Press, Taylor & Francis Group: Boca Raton, Fla, 2017; .

15. Harvey, J. D.; Jena, P. V.; Baker, H. A.; Zerze, G. H.; Williams, R. M.; Galassi, T. V.; Roxbury, D.; Mittal, J.; Heller, D. A. A carbon nanotube reporter of microRNA hybridization events in vivo. *Nature Biomedical Engineering* **2017**, *1*.

16. Szabó, A.; Perri, C.; Csató, A.; Giordano, G.; Vuono, D.; Nagy, J. B. Synthesis Methods of Carbon Nanotubes and Related Materials. *Materials* **2010**, *3*, 3092-3140.

17. Keidar, M.; Waas, A. M. On the conditions of carbon nanotube growth in the arc discharge. *Nanotechnology* **2004**, *15*, 1571-1575.

18. Bernier, P.; Journet, C.; Lefrant, S.; Deniard, P.; Fischer, J. E.; Loiseau, A.; de la Chapelle, M. Lamy; Lee, R.; Maser, W. K. Large-scale production of single-walled carbon nanotubes by the electric-arc technique. *Nature* **1997**, *388*, 756-758.

19. Eatemadi, A.; Daraee, H.; Karimkhanloo, H.; Kouhi, M.; Zarghami, N.; Akbarzadeh, A.; Abasi, M.; Hanifehpour, Y.; Joo, S. Carbon nanotubes: properties, synthesis, purification, and medical applications. *Nanoscale Res Lett* **2014**, *9*, 1-13.

20. Nitin Choudhary, Sookhyun Hwang, and Wonbong Choi *Carbon Nanomaterials: A Review;* Book collections on Project MUSE. Princeton University Press: 2018; .

21. Bronikowski, M. J.; Willis, P. A.; Colbert, D. T.; Smith, K. A.; Smalley, R. E. In *In Gas-phase production of carbon single-walled nanotubes from carbon monoxide via the HiPco process: A parametric study;* Jul 2001; Vol. 19, pp 1800-1805.

22. Tang, M. S. Y.; Ng, E.; Juan, J. C.; Ooi, C. W.; Ling, T. C.; Woon, K. L.; Show, P. L. Metallic and semiconducting carbon nanotubes separation using an aqueous two-phase separation technique: a review. *Nanotechnology* **2016**, *27*, 332002.

23. Tang, M. S. Y.; Ng, E.; Juan, J. C.; Ooi, C. W.; Ling, T. C.; Woon, K. L.; Show, P. L. Metallic and semiconducting carbon nanotubes separation using an aqueous two-phase separation technique: a review. *Nanotechnology* **2016**, *27*, 332002.

24. Duan, W. H.; Wang, Q.; Collins, F. Dispersion of carbon nanotubes with SDS surfactants: a study from a binding energy perspective. *Chemical Science* **2011**, *2*, 1407.

25. O'Connell, M. J.; Bachilo, S. M.; Huffman, C. B.; Moore, V. C.; Strano, M. S.; Haroz, E. H.; Rialon, K. L.; Boul, P. J.; Noon, W. H.; Kittrell, C.; Ma, J.; Hauge, R. H.; Weisman, R. B.; Smalley, R. E. Band Gap Fluorescence from Individual Single-Walled Carbon Nanotubes. *Science* **2002**, *297*, 593-596.

26. Kruss, S.; Hilmer, A. J.; Zhang, J.; Reuel, N. F.; Mu, B.; Strano, M. S. Carbon nanotubes as optical biomedical sensors. *Advanced Drug Delivery Reviews* **2013**, *65*, 1933-1950.

27. Karousis, N.; Tagmatarchis, N.; Tasis, D. Current Progress on the Chemical Modification of Carbon Nanotubes. *Chemical Reviews* **2010**, *110*, 5366-5397.

28. Dai, H.; Chen, Z.; Liu, Z.; Tabakman, S. M. Preparation of carbon nanotube bioconjugates for biomedical applications. *Nature Protocols* **2009**, *4*, 1372-1381.

29. Chattopadhyay, J.; de Jesus Cortez, F.; Chakraborty, S.; Slater, N. K. H.; Billups, W. E. Synthesis of Water-Soluble PEGylated Single-Walled Carbon Nanotubes. *Chemistry of Materials* **2006**, *18*, 5864-5868.

30. Gromov, A.; Dittmer, S.; Svensson, J.; Nerushev, O. A.; Perez-García, S. A.; Licea-Jiménez, L.; Rychwalski, R.; Campbell, E. E. B. Covalent amino-functionalisation of single-wall carbon nanotubes. *Journal of Materials Chemistry* **2005**, *15*, 3334-3339.

31. Zhang, W.; Swager, T. M. Functionalization of Single-Walled Carbon Nanotubes and Fullerenes via a Dimethyl Acetylenedicarboxylate−4-Dimethylaminopyridine Zwitterion Approach. *Journal of the American Chemical Society* **2007**, *129*, 7714-7715.

32. Zhao, Y.; Stoddart, J. F. Noncovalent Functionalization of Single-Walled Carbon Nanotubes. *Accounts of Chemical Research* **2009**, *42*, 1161-1171.

33. Haggenmueller, R.; Rahatekar, S. S.; Fagan, J. A.; Chun, J.; Becker, M. L.; Naik, R. R.; Krauss, T.; Carlson, L.; Kadla, J. F.; Trulove, P. C.; Fox, D. F.; DeLong, H. C.; Fang, Z.; Kelley, S. O.; Gilman, J. W. Comparison of the Quality of Aqueous Dispersions of Single Wall Carbon Nanotubes Using Surfactants and Biomolecules. *Langmuir* **2008**, *24*, 5070-5078.

34. Doig, J.; Nish, A.; Hwang, J.; Nicholas, R. J. Highly selective dispersion of single-walled carbon nanotubes using aromatic polymers. *Nature Nanotechnology* **2007**, *2*, 640-646.

35. O'Connell, M. J.; Boul, P.; Ericson, L. M.; Huffman, C.; Wang, Y.; Haroz, E.; Kuper, C.; Tour, J.; Ausman, K. D.; Smalley, R. E. Reversible water-solubilization of single-walled carbon nanotubes by polymer wrapping. *Chemical Physics Letters* **2001**, *342*, 265-271.

36. Zheng, M.; Jagota, A.; Tassi, N. G.; Diner, B. A.; Semke, E. D.; Lustig, S. R.; Mclean, R. S.; Richardson, R. E. DNA-assisted dispersion and separation of carbon nanotubes. *Nature Materials* **2003**, *2*, 338-342.

37. Ostojic, G. N.; Ireland, J. R.; Hersam, M. C. Noncovalent Functionalization of DNA-Wrapped Single-Walled Carbon Nanotubes with Platinum-Based DNA Cross-Linkers. *Langmuir* **2008**, *24*, 9784-9789.

38. Jeng, E. S.; Moll, A. E.; Roy, A. C.; Gastala, J. B.; Strano, M. S. Detection of DNA Hybridization Using the Near-Infrared Band-Gap Fluorescence of Single-Walled Carbon Nanotubes. *Nano Letters* **2006**, *6*, 371-375.

39. Zheng, M.; Jagota, A.; Tassi, N. G.; Diner, B. A.; Semke, E. D.; Lustig, S. R.; Mclean, R. S.; Richardson, R. E. DNA-assisted dispersion and separation of carbon nanotubes. *Nature Materials* **2003**, *2*, 338-342.

40. Budhathoki-Uprety, J.; Shah, J.; Korsen, J. A.; Wayne, A. E.; Galassi, T. V.; Cohen, J. R.; Harvey, J. D.; Jena, P. V.; Ramanathan, L. V.; Jaimes, E. A.; Heller, D. A. Synthetic molecular recognition nanosensor paint for microalbuminuria. *Nature communications* **2019**, *10*, 3605-9.

41. Dinarvand, M.; Neubert, E.; Meyer, D.; Selvaggio, G.; Mann, F. A.; Erpenbeck, L.; Kruss, S. Near-Infrared Imaging of Serotonin Release from Cells with Fluorescent Nanosensors. *Nano letters* **2019**, *19*, 6604-6611.

42. Ahn, J.; Kim, J.; Reuel, N. F.; Barone, P. W.; Boghossian, A. A.; Zhang, J.; Yoon, H.; Chang, A. C.; Hilmer, A. J.; Strano, M. S. Label-Free, Single Protein Detection on a Near-

Infrared Fluorescent Single-Walled Carbon Nanotube/Protein Microarray Fabricated by Cell-Free Synthesis. *Nano Letters* **2011**, *11*, 2743-2752.

43. Salem, D. P.; Gong, X.; Lee, H.; Zeng, A.; Xue, G.; Schacherl, J.; Gibson, S.; Strano, M. S. Characterization of Protein Aggregation Using Hydrogel-Encapsulated nIR Fluorescent Nanoparticle Sensors. *ACS sensors* **2020**, *5*, 327-337.

44. Harvey, J. D.; Williams, R. M.; Tully, K. M.; Baker, H. A.; Shamay, Y.; Heller, D. A. An in Vivo Nanosensor Measures Compartmental Doxorubicin Exposure. *Nano letters* **2019**, *19*, 4343-4354.

45. Jin, H.; Heller, D. A.; Kalbacova, M.; Kim, J.; Zhang, J.; Boghossian, A. A.; Maheshri, N.; Strano, M. S. Detection of single-molecule H2O2 signalling from epidermal growth factor receptor using fluorescent single-walled carbon nanotubes. *Nature nanotechnology* **2010**, *5*, 302-309.

46. Wu, H.; Nißler, R.; Morris, V.; Herrmann, N.; Hu, P.; Jeon, S.; Kruss, S.; Giraldo, J. P. Monitoring Plant Health with Near-Infrared Fluorescent H2O2 Nanosensors. *Nano Letters* **2020**, *20*, 2432-2442.

47. Gillen, A. J.; Siefman, D. J.; Wu, S.; Bourmaud, C.; Lambert, B.; Boghossian, A. A. Templating colloidal sieves for tuning nanotube surface interactions and optical sensor responses. *Journal of Colloid And Interface Science* **2020**, *565*, 55-62.

48. Salem, D. P.; Gong, X.; Liu, A. T.; Akombi, K.; Strano, M. S. Immobilization and Function of nIR-Fluorescent Carbon Nanotube Sensors on Paper Substrates for Fluidic Manipulation. *Analytical chemistry (Washington)* **2020**, *92*, 916-923.

49. Zhou, L.; Matsumura, H.; Mezawa, M.; Takai, H.; Nakayama, Y.; Mitarai, M.; Ogata, Y. Protamine stimulates bone sialoprotein gene expression. *Gene* **2013**, *516*, 228-237.

50. Fukushima, T.; Ohno, J.; Imayoshi, R.; Mori, N.; Sakagami, R.; Mitarai, M.; Hayakawa, T. DNA/protamine complex paste for an injectable dental material. *J Mater Sci: Mater Med* **2011**, *22*, 2607-2615.

51. Nemeno, J. G. E.; Lee, S.; Yang, W.; Lee, K. M.; Lee, J. I. Applications and Implications of Heparin and Protamine in Tissue Engineering and Regenerative Medicine. *BioMed research international* **2014**, *2014*, 936196-10.

52. Bakchoul, T. Protamine (heparin)-induced thrombocytopenia: a review of the serological and clinical features associated with anti-protamine/heparin antibodies. **2016**.

53. Awotwe-Otoo, D.; Agarabi, C.; Faustino, P. J.; Habib, M. J.; Lee, S.; Khan, M. A.; Shah, R. B. Application of quality by design elements for the development and optimization of an analytical method for protamine sulfate. *Journal of Pharmaceutical and Biomedical Analysis* **2012**, *62*, 61-67.

54. Egawa, Y.; Hayashida, R.; Seki, T.; Anzai, J. Fluorometric determination of heparin based on self-quenching of fluorescein-labeled protamine. *Talanta* **2008**, *76*, 736-741.

55. Wang, E.; Wang, G.; Ma, L.; Stivanello, C. M.; Lam, S.; Patel, H. Optical films for protamine detection with lipophilic dichlorofluorescein derivatives. *Analytica Chimica Acta* **1996**, *334*, 139-147.

56. Shvarev, A.; Bakker, E. Response Characteristics of a Reversible Electrochemical Sensor for the Polyion Protamine. *Analytical Chemistry* **2005**, *77*, 5221-5228.

57. Liu, Y.; Zhang, F.; He, X.; Ma, P.; Huang, Y.; Tao, S.; Sun, Y.; Wang, X.; Song, D. A novel and simple fluorescent sensor based on AgInZnS QDs for the detection of protamine and trypsin and imaging of cells. *Sensors & Actuators: B. Chemical* **2019**, *294*, 263-269.

58. Haggenmueller, R.; Rahatekar, S. S.; Fagan, J. A.; Chun, J.; Becker, M. L.; Naik, R. R.; Krauss, T.; Carlson, L.; Kadla, J. F.; Trulove, P. C.; Fox, D. F.; DeLong, H. C.; Fang, Z.; Kelley, S. O.; Gilman, J. W. Comparison of the Quality of Aqueous Dispersions of Single Wall Carbon Nanotubes Using Surfactants and Biomolecules. *Langmuir* **2008**, *24*, 5070-5078.

59. Daniel A. Heller; George W. Pratt; Jingqing Zhang; Nitish Nair; Adam J. Hansborough; Ardemis A. Boghossian; Nigel F. Reuel; Paul W. Barone; Michael S. Strano Peptide secondary structure modulates single-walled carbon nanotube fluorescence as a chaperone sensor for nitroaromatics. *Proceedings of the National Academy of Sciences of the United States of America* **2011**, *108*, 8544-8549.

60. Ishibashi, A.; Nakashima, N. Strong Chemical Structure Dependence for Individual Dissolution of Single-Walled Carbon Nanotubes in Aqueous Micelles of Biosurfactants. *Bulletin of the Chemical Society of Japan* **2006**, *79*, 357-359.

61. Roxbury, D.; Jena, P. V.; Shamay, Y.; Horoszko, C. P.; Heller, D. A. Cell Membrane Proteins Modulate the Carbon Nanotube Optical Bandgap via Surface Charge Accumulation. *ACS Nano* **2016**, *10*, 499-506.

APPENDICES

Appendix A

Normal suspension of SWCNTs

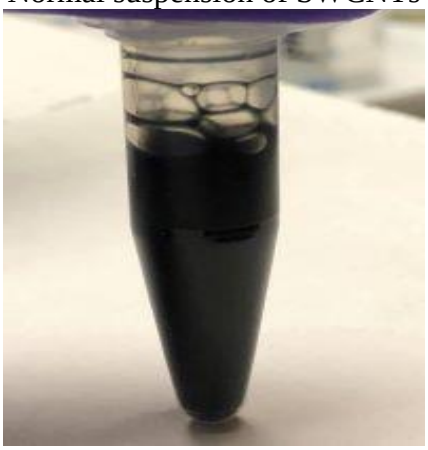

Aggregation of SWCNT

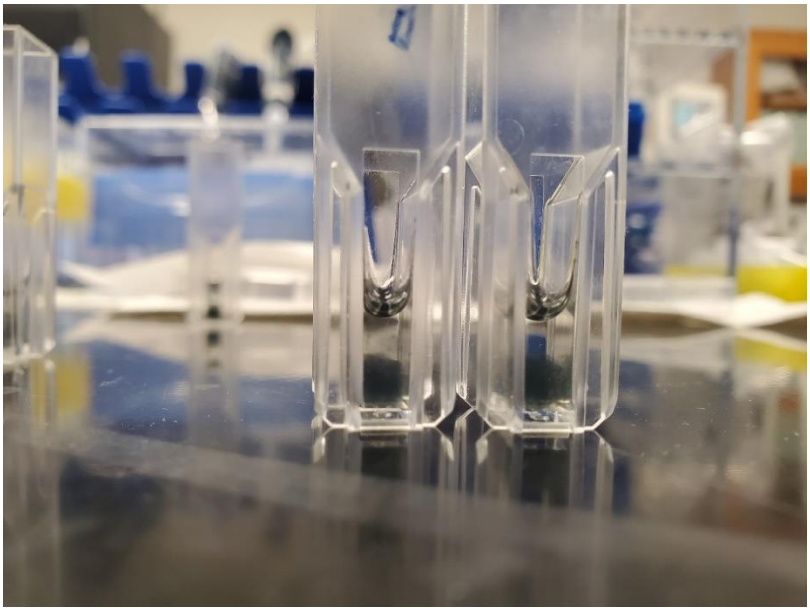

Appendix B

UV-vis-NIR absorption spectrum of PSS- (6,5) SWCNT